Frontiers of Information Technology & Electronic Engineering
www.jzus.zju.edu.cn; engineering.cae.cn; www.springerlink.com
ISSN 2095-9184 (print); ISSN 2095-9230 (online)
E-mail: jzus@zju.edu.cn

Review:

Classical and state-of-the-art approaches for underwater image defogging: a comprehensive survey*

Jing-chun ZHOU, De-huan ZHANG, Wei-shi ZHANG‡

College of Information Science and Technology, Dalian Maritime University, Dalian 116026, China

E-mail: {zhoujingchun, zhangdehuan, teesiv}@dlmu.edu.cn

Received Apr. 23, 2020; Revision accepted July 12, 2020; Crosschecked Nov. 11, 2020

Abstract: In underwater scenes, the quality of the video and image acquired by the underwater imaging system suffers from severe degradation, influencing target detection and recognition. Thus, restoring real scenes from blurred videos and images is of great significance. Owing to the light absorption and scattering by suspended particles, the images acquired often have poor visibility, including color shift, low contrast, noise, and blurring issues. This paper aims to classify and compare some of the significant technologies in underwater image defogging, presenting a comprehensive picture of the current research landscape for researchers. First we analyze the reasons for degradation of underwater images and the underwater optical imaging model. Then we classify the underwater image defogging technologies into three categories, including image restoration approaches, image enhancement approaches, and deep learning approaches. Afterward, we present the objective evaluation metrics and analyze the state-of-the-art approaches. Finally, we summarize the shortcomings of the defogging approaches for underwater images and propose seven research directions.

Key words: Underwater image defogging; Restoration approaches; Enhancement approaches; Evaluation metrics
https://doi.org/10.1631/FITEE.2000190 **CLC number:** TP391.4

1 Introduction

Nowadays, the environments that offer global resources face increasingly harsher restrictions, yet the ocean contains extensive sources of minerals and energy: this leads to a greater importance and strategic significance for the exploitation of marine resources (Han M et al., 2020). Since underwater images are an important medium in the acquisition of marine information, the visual quality of these images directly influences their practical applications (Pan et al., 2019; You et al., 2020). Owing to the complex imaging scenarios, the images obtained easily degenerate because of the suspended particles. The degenerated images present low contrast, blurring, color distortions, noise, and halos (Li YJ et al., 2018). The degenerated underwater images severely restrict practical applications such as feature extraction, target detection, and feature matching (Mangeruga et al., 2018; Zhao MH et al., 2019).

To obtain high-quality images for practical applications, researchers usually take the following measures, which have been extensively applied in many marine resource fields, to improve the visibility of underwater videos and images (Zhou et al., 2019a): improving underwater imaging environments, modifying underwater monitoring sensors, and providing stable transmission channels. However, the above-mentioned measures are costly and limited in practical applications (Zhou et al., 2019a). Compared with the high-cost hardware, applying low-cost digital

‡ Corresponding author

* Project supported by the National Natural Science Foundation of China (No. 61702074), the Liaoning Provincial Natural Science Foundation of China (No. 20170520196), and the Fundamental Research Funds for the Central Universities, China (Nos. 3132019205 and 3132019354)

ORCID: Jing-chun ZHOU, https://orcid.org/0000-0002-4111-6240; Wei-shi ZHANG, https://orcid.org/0000-0003-0519-8397

image processing software has a more practical value (Zhang WD et al., 2019a). As the key technologies in underwater image processing, restoration and enhancement approaches for underwater images have become a research hotspot, and the above-mentioned technologies have been extensively applied in the fields of marine resource survey, marine conservation, and the military (Hou et al., 2019). There are an important theoretical basis and practical significance for researchers to adopt image processing technology to enhance image quality.

To date, underwater optical imaging has been one of the challenging fields in computer vision research (Gao et al., 2019). Due to the limitations of the environment and the imaging equipment, the underwater images obtained have noise, blurring, and low contrast (Deng XY et al., 2019; Liu P et al., 2019). The ground-breaking research proposed by Duntley (1963) identified the limits for an underwater optical imaging model (UOIM). The UOIM (Jaffe, 1990) is shown in Fig. 1. The model has many limitations, which can be summarized as the following:

1. Low contrast and blurring of details: influenced by absorption and scattering, light represents exponential decay, leading to low contrast and blurring of details in the images obtained.

2. Color distortion: different from land imaging, different types of light have different attenuation rates in water due to the unique underwater environment and light conditions. The attenuation of light causes underwater images to be bluish or greenish (Marques et al., 2019). The selective attenuation model for underwater light is shown in Fig. 2. In visible light, red light at a comparatively large wavelength has the weakest penetrability; when it reaches 5 m underwater, it is the first to disappear; at 10 m underwater, orange light disappears; at 20 m underwater, yellow light disappears; at 30 m underwater, green light is absorbed. Blue and green lights have smaller absorption attenuation coefficients in water and stronger penetrability; thus, underwater images usually appear to be blue-green.

3. Noise: due to underwater micro-particles and the quality problems of the sensor devices, the images obtained have noise.

4. Halo: in deep-sea scenes, since there is no compensation for atmospheric light, artificial light is needed as an auxiliary light. However, artificial lighting gives rise to uneven illumination, which leads to a situation where the images obtained have shadow or there is false contouring (Wang Y et al., 2019).

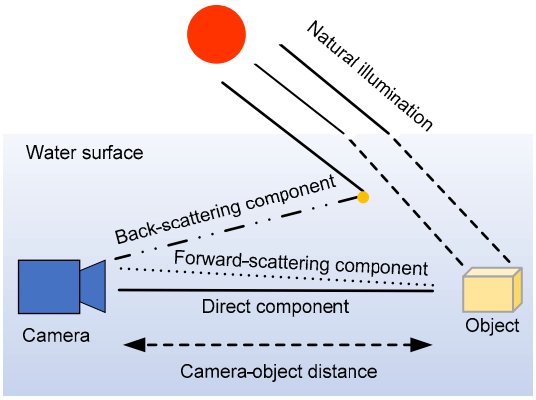

Fig. 1 Schematic of the underwater optical imaging model
Reprinted from Xie et al. (2018), Copyright 2018, with permission from MDPI, Basel, Switzerland, licensed under CC BY 4.0

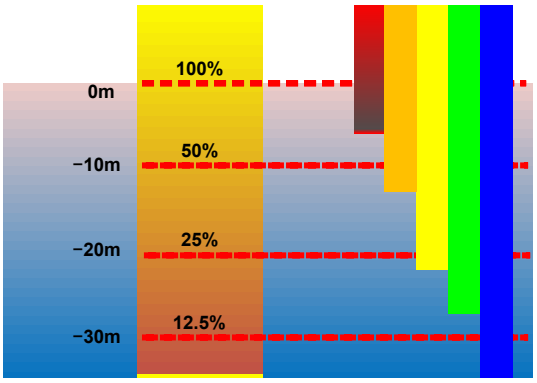

Fig. 2 Selective attenuation model of underwater light
Reprinted from Iqbal et al. (2007), Copyright 2007, with permission from the International Association of Engineers, licensed under CC BY 3.0

In conclusion, owing to the complexity of underwater scenarios and their attendant light sources, the transmission of light is influenced by medium absorption and scattering, severely degrading the quality of the collected underwater images. To apply computer vision technology to underwater imaging, underwater image defogging methods need to solve common problems: color casts, low contrast, noise, blurring of details, etc. The existing unambiguous approaches in underwater imaging can be divided into three categories: underwater image restoration approaches based on a physical model, underwater image enhancement approaches based on a nonphysical model, and approaches based on deep learning.

This paper presents a comprehensive survey of underwater image clarity technologies to help primary researchers determine the current developments in underwater image research, the existing problems, and promising applications. This paper also encourages researchers in the underwater imaging field to adopt underwater image processing technologies to help find practical solutions to the degradation of underwater images.

In this paper we analyze the UOIM, the unambiguous approaches to underwater images, and the existing problems. The contributions are presented as follows:

1. We introduce an underwater imaging model and reasons for degeneration of underwater images, including low contrast, blurring of details, color distortion, noise, and uneven illumination.

2. We classify and introduce the current unambiguous approaches for underwater images into three categories.

3. We test some representative approaches, analyzing the advantages and disadvantages of each approach from subjective and objective perspectives.

4. We present the characteristics and performances of and problems in the current approaches toward underwater image research, and provide seven research directions.

2 Jaffe-McGlamery underwater optical imaging model

The Jaffe-McGlamery UOIM (Jaffe, 1990) is as displayed in Fig. 1. The light received by the camera is linearly composed of three parts: direct component E_{d}, forward-scattering component E_{fs}, and back-scattering component E_{bs}.

The linear combination of these three components can be used to describe the underwater optical imaging model; the total irradiance E_{T} is

$$E_{\mathrm{T}}=E_{\mathrm{d}}+E_{\mathrm{fs}}+E_{\mathrm{bs}}. \tag{1}$$

E_{d} is the light directly reflected by the object, which does not scatter into the camera. Considering the effects of absorption and scattering, part of the light can be received by the camera (Nomura et al., 2018), and E_{d} is defined as

$$E_{\mathrm{d}}=J(m,\,n)\cdot t(m,\,n), \tag{2}$$

where $(m,\,n)$ represents the pixel coordinates of the image, $J(m,\,n)$ denotes scene radiance, and $t(m,\,n)$ indicates the transmission map (TM).

E_{fs} is the light reflected by the object entering the camera at a small angle. E_{fs} can be expressed as the convolution of E_{d} and a point spread function, which is defined as

$$E_{\mathrm{fs}}=J(m,\,n)*k(m,\,n), \tag{3}$$

where $k(m,\,n)$ indicates the convolution kernel function, which means the light scattering caused by forward scattering, and * is the convolution operation.

E_{bs} is the light that enters the camera after scattering by water or suspended particles. E_{bs} is defined as

$$E_{\mathrm{bs}}=(1-t(m,\,n))\cdot A^{\lambda}, \tag{4}$$

where A^{λ} denotes the background light (BL).

In most cases, because the distance from the object to the camera is short, forward scattering can be ignored. The UOIM can be simplified as

$$U^{\lambda}(m,\,n)=J^{\lambda}(m,\,n)\cdot t^{\lambda}(m,\,n)+(1-t^{\lambda}(m,\,n))\cdot A^{\lambda}, \tag{5}$$

where $U^{\lambda}(m,\,n)$ represents the collected underwater image, $\lambda\in\{\mathrm{r},\,\mathrm{g},\,\mathrm{b}\}$, $J^{\lambda}(m,\,n)\cdot t^{\lambda}(m,\,n)$ is the direct component, and $(1-t^{\lambda}(m,\,n))\cdot A^{\lambda}$ denotes the back-scattered component.

To collect a clear image, the estimation of $J^{\lambda}(i,j)$, $t^{\lambda}(i,\,j)$, and A^{λ} is of great significance. The estimated A^{λ} is substituted by the brightest pixel in $I^{\lambda}(i,j)$, which is

$$A^{\lambda}=\max_{x\in I}\left(\min_{y\in\Omega(m,n)}\left(\min_{\lambda}\left(I^{\lambda}(i,j)\right)\right)\right)=0, \tag{6}$$

where $\Omega(m,\,n)$ indicates a square local patch, which centers on pixel $(m,\,n)$, and λ represents the RGB color channel.

3 Underwater image defogging approaches

In recent years, researchers have proposed many underwater image defogging methods. A broad

categorization of the underwater image defogging approaches is given in Fig. 3. The underwater defogging approaches used to improve the visual quality of underwater images can be classified into underwater image restoration approaches based on a physical model, underwater image enhancement approaches based on nonphysical models, and approaches based on deep learning (Zhang WD et al., 2019b).

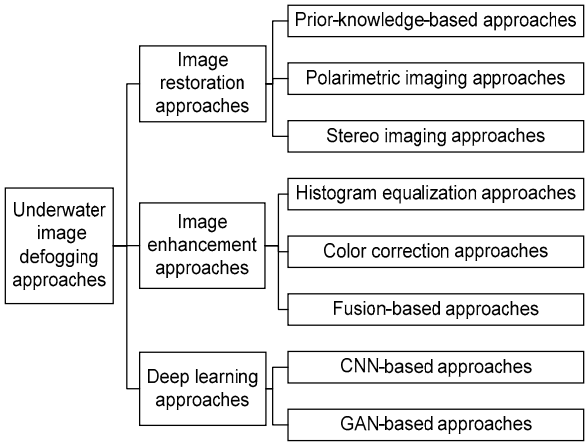

Fig. 3 Categories of underwater image defogging approaches

The underwater image enhancement methods based on nonphysical models do not need to consider the underwater imaging model; they need only the spatial relationships between pixel values to enhance the image contrast and color. For early underwater image enhancement, usually defogging methods were applied directly to the processing of underwater images. Later, underwater image enhancement methods were designed to address problems of blurring of degraded underwater images, low contrast, and color cast according to the UOIM, and these methods achieved the enhancement by changing the pixel value. Recently, approaches based on deep learning models, in particular, convolutional neural networks (CNNs) and generative adversarial networks (GANs), have been used to sharpen underwater images, and these methods enhanced image quality by learning to hide certain characteristics (Abu and Diamant, 2019).

3.1 Underwater image restoration approaches

Underwater image restoration approaches based on physical models aim to reduce the effects produced by the underwater environment. Most methods are based on the Jaffe-McGlamery model (McGlamery, 1980). This model is a sophisticated underwater optical imaging system, which uses the prior knowledge of the image and model parameters to reconstruct the real underwater scenes (Jaffe, 1990). This subsection analyzes the underwater image restoration methods in detail from three aspects, prior-knowledge-based approaches, polarimetric imaging approaches, and stereo imaging approaches.

Prior-knowledge-based approaches are a representative of software-based methods. They can effectively achieve underwater image defogging. The software methods introduced here are dark channel prior (DCP) and DCP-based variants. In general, these methods are based on assumptions about different coefficients, which may not be sufficiently accurate. Compared with hardware-based methods, software-based methods simplify modulation, reduce the investment cost, and are easy to use.

Polarimetric imaging methods and stereo imaging methods are regarded as hardware-based imaging methods. These underwater image defogging methods use hardware for underwater image restoration. The hardware devices used are sensors, polarizers, and stereo imaging equipment.

Polarization imaging technology uses polarized light sources or polarized cameras to capture underwater images. To a certain extent, it can reduce the impact of suspended particles and back-scattered light, which can improve the contrast in underwater images. Stereo imaging technology puts a stereo camera on the seabed to capture images.

Hardware-based underwater image defogging methods do not need to consider a priori knowledge of the imaging environment, and simply use physical hardware equipment to improve the visual quality of the images. Most of these methods are easy to implement and have low computational complexity. However, the degradation of the underwater image is not considered, and this is the essential reason that the processing result does not necessarily represent the true appearance of the image, that the details of the image are not sufficiently enhanced, and that the processed image has obvious noise amplification problems.

3.1.1 Prior-knowledge-based approaches

DCP technology is an effective defogging method based on the Jaffe-McGlamery model. The

flowchart of the DCP defogging method can be seen in Fig. 4. The aim of this model is to improve the accuracy in the estimated BL and TM (Singh and Kumar, 2019).

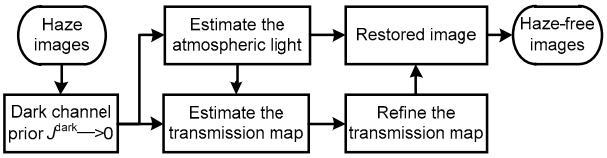

Fig. 4 The dark channel prior (DCP) defogging model

DCP was designed by He KM et al. (2009), and it can be used to effectively estimate the TM. Many researchers have made improvements based on the DCP model, including Drews et al. (2013) and Wen et al. (2013). However, they calculated only the dark channel in the blue and green channels:

$$J_{\text{udark}}^{\lambda'}(m,n)=\min_{\lambda'\in\{\text{g,b}\}}\left(\min_{y\in\Omega(m,n)}\left(\frac{J^{\lambda'}(y)}{A^{\lambda'}}\right)\right)$$
$$=t^{\lambda'}(m,n)\min_{\lambda'}\left(\min_{y}\left(\frac{J^{\lambda'}(y)}{A^{\lambda'}}\right)\right)+(1-t^{\lambda'}(m,n))\to 0. \tag{7}$$

Based on Eqs. (5) and (7), the TM $t^{\lambda'}(m,n)$ is

$$t^{\lambda'}(m,n)=1-\min_{\lambda'}\left(\min_{y}\left(\frac{I^{\lambda'}(y)}{A^{\lambda'}}\right)\right). \tag{8}$$

The final result $F(m, n)$ is

$$F(m,n)=\frac{I^{\lambda'}(m,n)-A^{\lambda'}}{\max(t^{\lambda'}(m,n),t_0)}+A^{\lambda'}. \tag{9}$$

When $t^{\lambda'}(m,n)$ is close to 0, the direct transmission part will be very close to 0. Directly restoring this part of the scene may amplify the noise in this area, so we need to set a minimum value for the transmission rate t_0; usually, the value is 0.1.

The restoration method based on prior information needs to extract physical properties through the prior knowledge and hypotheses, and then estimates the BL and TM using these properties to restore an underwater image. There are several variants of TM and BL estimation approaches, as listed in Table 1 (Yang M et al., 2019). Compared with the land environment, in the underwater environment, DCP is more likely to be influenced by light attenuation. Thus, some researchers improved and expanded DCP based on the underwater physical properties.

Chao and Wang (2010) eliminated the influence of scattering and restored underwater images using the DCP method. However, the restored images were not satisfactory, as their method may also lead to color distortions. An easily implemented enhancement approach based on DCP for underwater images was proposed by Yang HY et al. (2011). The airlight was estimated by DCP, and the depth map was generated using the median filter. The highest blue color channel was set as the average target value. It can balance the red and green channels and achieve color correction. However, the method cannot solve the color cast when the image appears green. Therefore, Chiang and Chen (2012) combined the wavelength compensation and image dehazing (WCID) algorithm with the classical DCP defogging method, considering artificial light, the scattering effect of the transmission path, and the influence of color attenuation for the first time. This method can better restore the blue-color images, eliminating the effect of artificial light. Yet, when processing images with a severe color cast problem, the method is invalid. Based on the UOIM, Zhao XW et al. (2015) proposed a defogging approach without requiring camera parameters or underwater optical properties in advance. The transmission of three color channels was estimated separately based on DCP, through the relationship between the global BL of underwater images and the inherent optical properties. To reduce information loss in the output images, Li CY et al. (2016) introduced a restoration algorithm using the minimum information loss principle and underwater optical imaging characteristics. This method generates two enhanced underwater images simultaneously. One image has a realistic appearance and natural color, and the other has higher contrast and brightness. This approach does not require to obtain multiple images and complex information in the same scenario.

When light is transmitting in water, compared with blue light and green light, red light has a larger wavelength and lower frequency, and it is attenuated more quickly in water. Thus, red light is defined as the dark channel. Galdran et al. (2015) provided a red channel approach (RCP), which restores colors that are related to a smaller wavelength, and this can be

Table 1 Mathematical formulas for background light (BL) and transmission map (TM) estimation

Reference	BL estimation	TM estimation	Prior
Carlevaris-Bianco et al. (2010)	$\tilde{A}^{\lambda}=I^{\lambda}(\arg\min_{(i,j)}(\tilde{t}^{\lambda}(i,j)))$	$\tilde{t}^{\lambda}(i,j)=D_{\mathrm{mip}}(i,j)+(1-\max_{(i,j)}D_{\mathrm{mip}}(i,j))$	D_{mip}
Chao and Wang (2010)	$\tilde{A}^{\lambda}=I^{\lambda}(\arg\max_{(i,j)}(P(i,j)))$	$\tilde{t}^{\lambda}(i,j)=1-\min_{\lambda\in\{\mathrm{r,g,b}\}}(\min_{y\in\Omega(i,j)}(I^{\lambda}(y)\tilde{A}^{\lambda}))$	$I^{\lambda}_{\mathrm{dark}}$
Yang HY et al. (2011)	$\tilde{A}^{\lambda}=I^{\lambda}(\arg\max_{(i,j)\in p_{0.1\%}}\sum_{k\in\{\mathrm{r,g,b}\}}I^{k}(i,j))$	$\tilde{t}^{\mathrm{r}}(i,j)=1-\min_{k\in\{\mathrm{r,g,b}\}}(\operatorname{med}_{y\in\Omega(i,j)}(I^{k}(y)/\tilde{A}^{k}))$	$I^{\lambda}_{\mathrm{dark}}$
Chiang and Chen (2012)	$\tilde{A}^{\lambda}=I^{\lambda}(\arg\max_{(i,j)}(I^{\lambda}_{\mathrm{dark}}(i,j)))$	$\tilde{t}^{\lambda}(i,j)=1-\min_{\lambda\in\{\mathrm{r,g,b}\}}(\min_{y\in\Omega(i,j)}(I^{\lambda}(y)/\tilde{A}^{\lambda}))$ $\tilde{t}^{\lambda'}(i,j)=(\tilde{t}^{\lambda}(i,j))^{\beta^{\lambda'}/\beta^{\lambda}}$	$I^{\lambda}_{\mathrm{dark}}$
Wen et al. (2013)	$\tilde{A}^{\lambda}=I^{\lambda}(\arg\min_{(i,j)}(I^{r}(i,j)-\max_{(i,j)}(I^{\lambda'}_{\mathrm{dark}}(i,j))))$	$\tilde{t}^{\lambda'}(i,j)=1-\min_{\lambda'\in\{\mathrm{g,b}\}}(\min_{y\in\Omega(i,j)}(I^{\lambda'}(y)/\tilde{A}^{\lambda'}))$ $\tilde{t}^{\mathrm{r}}(i,j)=\tau\max_{y\in\Omega(i,j)}(I^{\mathrm{r}}(y)),\ \tau=\frac{\operatorname{avg}_{(i,j)}(\tilde{t}^{\lambda'}(i,j))}{\operatorname{avg}(\max_{(i,j)}\max_{y\in\Omega(i,j)}I^{\mathrm{r}}(y))}$	$I^{\lambda'}_{\mathrm{dark}}$
Drews et al. (2013)	$\tilde{A}^{\lambda'}=I^{\lambda}(\arg\max_{(i,j)}(I^{\lambda'}_{\mathrm{dark}}(i,j)))$	$\tilde{t}^{\lambda'}(i,j)=1-\min_{\lambda'\in\{\mathrm{g,b}\}}\left(\min_{y\in\Omega(i,j)}\left(\frac{I^{\lambda'}_{\mathrm{dark}}(y)}{\tilde{A}^{\lambda'}}\right)\right)$	$I^{\lambda'}_{\mathrm{dark}}$
Galdran et al. (2015)	$\tilde{A}^{\lambda}=I^{\lambda}(\arg\max_{(i,j)\in p_{10\%}}(I^{c}(i,j)))$	$\tilde{t}^{\lambda}(i,j)=1-\min_{\lambda\in\{\mathrm{r,g,b}\}}\left(\frac{\min_{y\in\Omega(i,j)}(1-I^{\mathrm{r}}(y))}{1-\tilde{A}^{\mathrm{r}}},\right.$ $\frac{\min_{y\in\Omega(i,j)}(I^{\mathrm{g}}(y))}{\tilde{A}^{\mathrm{g}}},\frac{\min_{y\in\Omega(i,j)}(I^{\mathrm{b}}(y))}{A^{\mathrm{b}}},$ $\left.\omega\min_{y\in\Omega(i,j)}\left(\frac{\max_{\lambda}(I^{\lambda}(i,j)-\min_{\lambda}(I^{\lambda}(i,j)))}{\max_{\lambda}(I^{\lambda}(i,j))}\right)\right)$	$I^{\mathrm{r'gb}}_{\mathrm{dark}}$
Peng et al. (2015)	$\tilde{A}^{\lambda}=\frac{1}{\lvert p_{0.1\%}\rvert}\sum_{(i,j)\in p_{0.1\%}}I^{\lambda}(i,j)$	$\tilde{t}^{\lambda}(i,j)=F_{\mathrm{s}}\{P_{\mathrm{b}}(i,j)\}$	$1-P_{\mathrm{b}}$
Zhao XW et al. (2015)	$\tilde{A}^{\lambda}=I^{\lambda}(\arg\max_{\lambda'\in\{\mathrm{g,b}\},(i,j)\in p_{0.1\%}}\lvert I^{\lambda}(i,j)-I^{\lambda'}(i,j)\rvert)$	$\tilde{t}^{\lambda}(i,j)=1-\min_{\lambda}(\min_{y\in\Omega(i,j)}(I^{\lambda}(y)/\tilde{A}^{\lambda}))$ $\tilde{t}^{\lambda'}(i,j)=(\tilde{t}^{\lambda}(i,j))^{\beta^{\lambda'}/\beta^{\lambda}}$	$I^{\lambda}_{\mathrm{dark}}$
Li CY et al. (2016)	$\tilde{A}^{\mathrm{b}}=I^{\lambda}(\arg\max_{(i,j)\in p_{0.1\%}}\lvert I^{\mathrm{r}}(i,j)-I^{\mathrm{b}}(i,j)\rvert)$ $\tilde{A}^{\mathrm{g}}=I^{\lambda}(\arg\max_{(i,j)\in p_{0.1\%}}\lvert I^{\mathrm{r}}(i,j)-I^{\mathrm{g}}(i,j)\rvert)$	$\tilde{t}^{\lambda'}(i,j)=(\tilde{t}^{\lambda}(i,j))^{\beta^{\lambda'}/\beta^{\lambda}}$	$I^{\lambda}_{\mathrm{dark}}$
Peng and Cosman (2017)	$\tilde{A}^{\lambda}=\alpha\tilde{A}^{\lambda}_{\max}+(1-\alpha)\tilde{A}^{\lambda}_{\min}$	$\tilde{t}^{\lambda}(i,j)=\mathrm{e}^{-\beta^{\lambda}\tilde{d}f(i,j)},\tilde{d}f(i,j)=D_{\infty}(\tilde{d}_{n}(i,j)+\tilde{d}_{0})$ $\tilde{d}_{n}(i,j)=\theta_{b}[\theta_{a}\tilde{d}_{D}(i,j)+(1-\theta_{a})\tilde{d}_{R}(i,j)]$ $+(1-\theta_{b})\tilde{d}_{B}(i,j)d_{0}=1-\max_{\lambda\in\{\mathrm{r,g,b}\}}\left(\frac{\lvert A^{\lambda}-I^{\lambda}(i,j)\rvert}{\max(\tilde{A}^{\lambda},1-\tilde{A}^{\lambda})}\right)$	$I^{\lambda}_{\mathrm{dark}}$
Song et al. (2018)	$\tilde{A}^{\lambda}=I^{\lambda}(\max_{(i,j)\in p_{0.1\%}}(d(i,j)))$	$\tilde{t}^{\lambda}(i,j)=\mathrm{Nrer}(\lambda)^{d(i,j)}$ $d(i,j)=\mathrm{ULAP}(i,j)$	D_{ULAP}
Pan et al. (2018)	$A^{\lambda'}=I^{\lambda'\in\{\mathrm{g,b}\}}(\arg\max_{(i,j)\in p_{0.1\%}}\sum_{\lambda'}I^{\lambda'}(i,j))$ $\tilde{A}^{\lambda}=\arg\max_{(i,j)\in p_{0.1\%}}\sum_{\lambda\in\{\mathrm{r}\}}I^{\lambda}(i,j)$	$\tilde{t}^{\lambda}(i,j)=\max(w^{(i,j)}*I^{\lambda}+b^{(i,j)})$	$I^{\lambda}_{\mathrm{dark}}$
Dai et al. (2020)	$\tilde{A}^{\lambda}=\frac{1}{3n}\sum_{\lambda\in\{\mathrm{r,g,b}\}}\sum_{x=1}^{n}I^{\lambda}_{k}(x)$ $+\frac{1}{n}\sum_{x=1}^{n}\lvert I^{\mathrm{b}}_{k}(x)-I^{\mathrm{r}}_{k}(x)\rvert+\lvert I^{\mathrm{g}}_{k}(x)-I^{\mathrm{r}}_{k}(x)\rvert$ $-\frac{1}{3}\sum_{\lambda\in\{\mathrm{r,g,b}\}}\sqrt{\frac{1}{n}\sum_{x=1}^{n}[I^{\lambda}_{k}(x)-\overline{I^{\lambda}_{k}}(x)]^{2}}$	$\tilde{t}^{\lambda}(i,j)=\frac{\lvert I^{\lambda}(y)-\tilde{A}^{\lambda}\rvert}{\max_{y\in\Omega(i,j)}\lvert I^{\lambda}(y)-\tilde{A}^{\lambda}\rvert}$	$I^{\lambda}_{\mathrm{dark}}$

explained as a variant of the DCP, adding prior saturation to DCP to process the artificial light. This method can effectively restore the lost contrast. Yet, this method considers only the red channel to measure the transmission, thus estimating the scene depth inaccurately, leading to poor restoration performance.

To remove the deviations caused by the red channel, a method to estimate BL and TM was proposed by Wen et al. (2013). This approach can handle the deep-sea images and images acquired from a turbid underwater environment. Drews et al. (2013) gave a method to estimate TM in a single underwater image, which assumes that the main sources of the underwater visual information are from the blue and green channels, while the underwater DCP (UDCP) cannot be successful when there exist white objects or artificial light. Based on depth-related colors, Peng et al. (2018) proposed the generalized DCP (GDCP), which calculates the difference between BL and the intensity of observation to estimate the environmental light and TM. When there is bright sand in the foreground in some underwater images, the sand will be mistaken as background using the DCP-based method; in this case, the precondition is not valid, and the methods that consider only the RGB channels may cause an error in scene depth estimation.

When the prior information is incorrect, methods based on prior information would usually result in large estimation errors. Normal underwater images lack reliable prior information, which has become a significant obstacle for this research orientation. Thus, besides the mentioned prior information, some other underwater restoration approaches have been used to restore images extensively.

As an alternative to DCP methods, Carlevaris-Bianco et al. (2010) introduced an algorithm for underwater image scene depth estimation, which is the maximum intensity prior (MIP) method. This approach estimates the TM using the difference between the maximum intensity of the R channel and the maximum intensity of the G and B channels, which is related to wavelength decay. When the difference between the attenuations in the RGB channels is little, light scattering cannot be removed, as stated by Peng et al. (2015), who proposed the blurriness prior (BP). The larger the depth of water, the vaguer the underwater objects, while the BP can conduct a depth estimation and restore the images. In another work by Peng and Cosman (2017), the image blurring and light absorption (IBLA) algorithm was proposed to improve the BP. This method combines hierarchical search and light transmission properties to estimate the global BL. It can more accurately estimate the BL and the depth of underwater scenes, and remove the effects of suspended particles and bright objects from many complicated scenes. Song et al. (2018) proposed an approach based on the underwater light attenuation prior (ULAP), which can effectively estimate the scene depth. It assumes that the scene depth is closely related to the difference between the maximum value of the G and B channels and the value of the R channel. Dai et al. (2020) proposed a method which decomposes the attenuation color curves to enhance single underwater images. The method includes BL research, TM calculation, and color balance, using a score formula and quadtree subdivision hierarchy search method to estimate BL, decomposing the decay curves on the RGB channels of underwater images to collect the TM, and using the bright channel balance to obtain images with a natural appearance.

In underwater scenes, some hypotheses of the DCP-based approaches are unreasonable. Since some parameters of the UOIM would undergo great changes due to the different environments, the estimation of parameters would influence the restoration results directly, and the key parameters of the UOIM, including BL and TM. A few famous underwater restoration technologies are presented in Table 1, including DCP, MIP, RCP, UDCP, BP, ULAP, IBLA, and DCAC. The mathematical models of these technologies have been applied to the estimation of scene depth extensively. Table 1 presents many BLs, TMs, and other prior estimation methods. In Table 1, $\lambda \in \{\mathrm{r}, \mathrm{g}, \mathrm{b}\}$, and $\lambda' \in \{\mathrm{g}, \mathrm{b}\}$; (i, j) represents the pixel coordinates; I^{λ} denotes the image for foggy days; $\tilde{A}^{\lambda}$ indicates the BL; $\tilde{t}^{\lambda}(i, j)$ denotes the TM; $D_{\mathrm{mip}}(i, j)$ is the difference between the maximum intensity of the R channel and G, B channels; ω represents the weight; b is the bias of the network; F_{s} is the soft matting; P_{b} denotes the refined blurriness map; $\Omega(i, j)$ indicates the local path which takes (i, j) as the central coordinates; $p_{0.1\%}$ represents the brightest pixels (top 0.1%) picked in $I^{\lambda}(i, j)$.

In Fig. 5, we compare several real underwater image restoration methods. Fig. 5a shows that degraded underwater images suffer from absorption and scattering. Figs. 5b–5h show a comparison of the results obtained using the restoration methods. The method from Chao and Wang (2010) shows no significant improvement in the restored images. It retains a bluish and greenish color cast. The method from Chiang and Chen (2012) could deal with defogging and color cast simultaneously. Due to the influence of suspended particles, the scene depth estimation is not accurate. Therefore, there are halo artifacts and path effects in the restored images. Figs. 5d–5h show the restoration results obtained on the raw underwater images using the methods of Drews et al. (2013), Li CY et al. (2016), Peng et al. (2015), Peng and Cosman (2017), and Song et al. (2018). We can see success in dehazing because the same image formation model is used. Drews et al. (2013) used the blue and green channels to estimate the TM, but it is not valid for some underwater images. The over-bright and over-dark areas are revealed in the restored images. The method from Li CY et al. (2016) can improve contrast and correct color distortion. The over-exposure appearance, however, remains. Figs. 5f and 5g are not as good as Fig. 5e. The selective attenuation of underwater light is ignored when estimating TMs and BL (Peng and Cosman, 2017). Fig. 5h shows that Song et al. (2018)'s method can effectively dehaze images, improve details, and achieve better visual performance in underwater scenarios.

3.1.2 Polarimetric imaging approaches

Polarization is an inherent attribute of light, and it can provide more valuable information than the scene spectrum (color) and intensity distribution. Images processed by polarization methods hold higher visual contrast than those processed by traditional images (Han PL et al., 2018). By collecting polarization images under different polarization states in the same scene, underwater polarization imaging technology accurately estimates the polarization characteristics (polarization degree or polarization angle) of back-scattering light, inverting the degeneration process, acquiring the background scattering light intensity and the transmission coefficient, and improving the clarity of images. Thus, this method has been applied extensively in the restoration of underwater images.

The schematic of the experimental setup for underwater imaging is depicted in Fig. 6. By simulating a real-world underwater imaging scenario, the

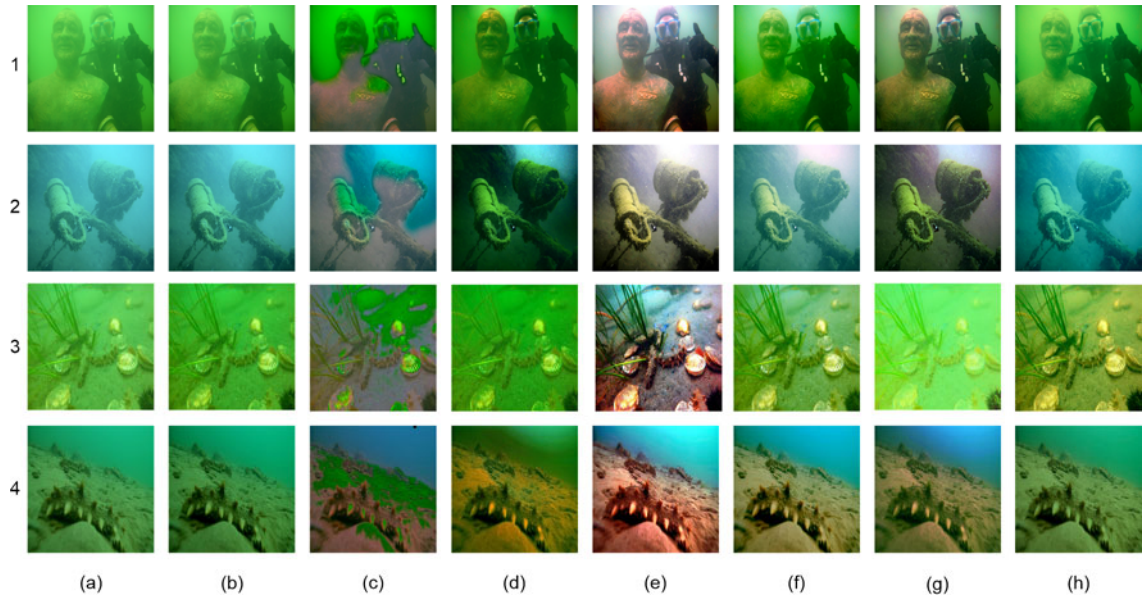

Fig. 5 Comparison of underwater image restoration methods: (a) underwater raw images; (b–h) images obtained using Chao and Wang (2010), Chiang and Chen (2012), Drews et al. (2013), Li CY et al. (2016), Peng et al. (2015), Peng and Cosman (2017), and Song et al. (2018)'s methods, respectively

Rows 1 and 2 are reprinted from the public data sets given by Li CY et al. (2019). References to color refer to the online version of this figure

polarization characteristics of the target object are estimated. The light source can be chosen as a light emitting diode (LED) lamp or laser source. The rotating polarizer is put in front of the charge-coupled device (CCD) camera as the analyzer. The light output from the lamp is reflected by the target object, and then through the rotating polarizer to impinge on the CCD camera. We fill the tank with clean water, and add different impurities to the water to make it turbid.

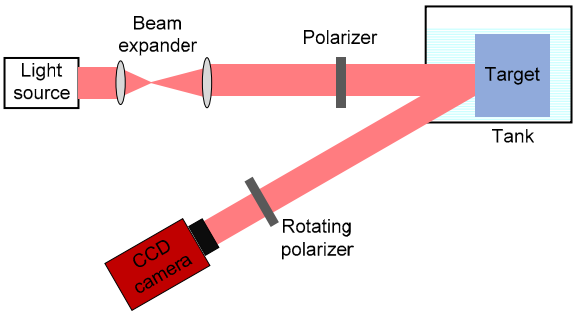

Fig. 6 Schematic of the experimental setup for underwater imaging

Schechner et al. (2001) proposed for the first time a defogging scheme based on polarization imaging to improve the clarity of foggy images. In recent years, this team and other researchers have been conducting further study on the theory and applying it to improve the quality of underwater images.

To recover the real scenes, Schechner et al. (2003) used specialized hardware equipment to collect many different polarization angle images in the same scene, calculating the scene depth through the relationship between polarization and back scattering. This method does not need a particular scattering model, but when the visibility is low or the light condition is poor, this method has poor performance. Schechner and Karpel (2005) proposed an image inverting model based on a polarization apparatus, collecting images from the target object at different angles. This method could restore the structural information of the scene without calculating the environment parameters or natural light, thus improving the visibility of the images. Yet, when collecting images from moving objects, it is hard to collect the same polarization images at the same time. Yemelyanov et al. (2006) proposed an adaptive algorithm for two-channel polarization sensing under various polarization statistics with nonuniform distributions. This algorithm uses principal component analysis to determine the best linear combination for the polarization channel, separating the polarization object from the background.

A preliminary study shows that polarization can modulate the back scattering (Giakos, 2004; Wu et al., 2020). Treibitz and Schechner (2006) proposed the instant 3Descatter, eliminating the rest of the back-scattering, and the 3D structure of a scene from the frames obtained by installing a polarization apparatus, to collect images in the light source and the camera. However, some parts of the hypothesis in this method are false. Thus, it is restricted in its applicability.

Because noise would influence the result of imaging, Schechner and Averbuch (2007) proposed an adaptive polarization smoothing method, which can restore the visibility and restrict the amplification of noise at the same time. Treibitz and Schechner (2009) obtained two polarization images at two orthogonal directions to restore the original scene, improving the image contrast. However, many unknown parameters (such as media attenuation coefficient and scene depth) cannot be accurately estimated. Treibitz and Schechner (2012) collected multidirectional illumination fusion of images under many artificial lights, which could solve problems of uneven illumination and partial low contrast, and collect clear underwater images. Xu et al. (2015) proposed a method for underwater light communication performance evaluation based on polarization information, analyzing the transmitting characteristics of polarization light under different water types and link distances. Huang BJ et al. (2016) proposed a method for underwater image recovery based on estimating the polarized difference (PD) image of the target signal. This method uses nonlinear calculation, but many parameters need to be optimized, which is time-consuming. Hu et al. (2017) proposed an underwater image restoration method based on adjustment of the TM. Without considering the polarization degree of objects, this method can significantly improve and optimize the quality of images. Hu et al. (2018) proposed an underwater image restoration method based on different position polarization degrees and the back-scattering intensity of underwater images under uneven illumination. This method can effectively

improve the quality of underwater images. Amer et al. (2019) combined the polarization imaging optical system with the optimized DCP method to significantly improve the quality of underwater images. Liu F et al. (2019) proposed an underwater polarization imaging model which considers the scattering and absorption effect of water. This model uses polarization information to estimate the target scene distance, removing the back-scattering problem. Then it uses the gray world assumption and the information of the image at a particular wavelength to adjust the color distortion caused by absorption.

To obtain the four-dimensional light field and polarization information by single imaging, Tian et al. (2019) proposed radiation of the object extraction method based on the polarization degree of the multi-view image and back-scattering intensity. This method can collect four-dimensional light field information and polarization information at the same time. Liu TG et al. (2020) proposed a method of polarimetric color image recovery in an underwater environment based on compensating for the crosstalk effect while estimating the transmittances of RGB channels. The proposed method can correctly estimate the transmission rate of RGB channels, enhancing the underwater image contrast and correcting color.

Using polarization-based methods can enhance visibility and estimate distance in scattering media. The formation of images under artificial illumination was studied by Treibitz and Schechner (2009). The method is simple, and the hardware is compact. Two images of the underwater scenario can be taken immediately by the camera with polarizers in different states. Fig. 7 shows an underwater image taken in the Mediterranean using artificial light sources and the corresponding de-scattered image.

(a) (b)

Fig. 7 Raw image (a) and de-scattered image (b)
Reprinted from Treibitz and Schechner (2006), Copyright 2006, with permission from IEEE

3.1.3 Stereo imaging approaches

In recent years, 3D image technology has embraced significant developments, but there are few defogging methods based on stereo imaging technology. Roser et al. (2014) proposed a stereo imaging method for autonomous underwater vehicles (AUVs), which estimates the visibility coefficients to restore underwater images (using stereo matching and a decaying light model to restore the underwater visibility). In an underwater environment of high turbidity, this method uses two stereograms under processing to improve the quality of the entire image. First, this method creates a rough 3D scene map from the degenerated stereogram, using the atmospheric scattering physical model under natural light to estimate visibility; then, it uses the optimized stereo map to estimate the visibility coefficients accurately and reconstruct the 3D scenes. This method evaluates experiment statistics collected from coastal waters at low visibility and with insufficient natural light using an AUV. This method can enhance underwater images in real time. However, in the shallow water, the stereo matching algorithm of this method has poor robustness. Lee et al. (2014) proposed a novel approach using stereo foggy-day images to extract defogged images. This method calculates the scattering coefficient and depth information to estimate the TM of the underwater image. It does not require prior knowledge, restrictions, or many images taken at different times. Nevertheless, because the estimated disparity layer appears as discontinuous phenomena in the far scenes, the structural information of natural scenes cannot be obtained.

Underwater image restoration approaches also have drawbacks. These approaches require physical models or specialized hardware equipment to improve the quality of the underwater images. Although these methods provide significant performances in the restoration of the visual effect of underwater images, there are still some problems affecting their applicability. For instance, these methods based on the imaging model need to collect many parameters, among which many will change with the change of scenes, which limits the application of physical models. Methods based on polarization imaging and stereo imaging require particular hardware equipment, which is expensive and complicated. The main disadvantage of underwater image restoration methods

based on physical models is the need for many calculation resources.

3.2 Underwater image enhancement approaches

Underwater image enhancement methods do not need the optical imaging model or any physical characteristics. The enhancement methods improve the visual effects in underwater images directly by nonlinear stretching of pixel values and an even distribution of the original histogram, which is distributed randomly. In recent years, researchers have proposed many underwater image enhancement methods, such as the histogram equalization method, color correction method, fusion method, and Retinex algorithm. These methods have been proved to work for the defogging of underwater images.

3.2.1 Histogram equalization approaches

Histogram indicates the distribution of the image tone (Chang et al., 2018). Histogram equalization is a typical image enhancement approach; it is used to solve the problem of low contrast. Compared with images acquired on land, the distribution of the underwater image pixel histogram is more concentrated. Thus, the dynamic range of image histograms is amplified to enhance the contrast of degenerated images (Kapoor et al., 2019).

Some researchers enhanced images by changing the distribution of the histogram (Hummel, 1977). As a typical enhancement approach, the histogram equalization method has attracted great attention from researchers. The researchers in this field improve the traditional histogram equalization method to achieve better enhancement of images. Pizer et al. (1987) proposed adaptive histogram equalization (AHE), which changes functions in the neighborhood to convert every pixel, optimizing the partial contrast of images effectively, but noise in the homogeneous region is enhanced. Kim TK et al. (1998) proposed a local histogram equalization (LHE), which highlights the image characteristics by defining image sub-blocks to conduct histogram equalization. LHE requires huge computation, and includes problems of blocking effect and color distortion. Kim YT (1997) proposed the brightness-preserving bi-histogram equalization (BBHE), which decomposes the image and makes the components of the decomposed images almost equal to the mean value. The BBHE method can enhance the image contrast while preserving its brightness. Compared with traditional histogram equalization methods, this method requires more sophisticated hardware. Reza (2004) proposed the contrast limited adaptive histogram equalization (CLAHE), which is an expansion of AHE, effectively restricting the amplification of noise, but the enhancement effect around the borders is poor. Tang JR and Isa (2017) proposed bi-histogram equalization using modified histogram bins (BHEMHB), which enhances the image details and the average brightness by minimizing the high-frequency bin. However, noise still exists in the enhanced images. Demirel and Anbarjafari (2011) proposed a restoration method by inverse discrete wavelet transform (IDWT), which conducts wavelet decomposition on images to acquire some subband images, and the subbands of high frequency and the original input image are interpolated, adjusting the coefficients obtained by the interpolation of high-frequency subband images through the changes in stable wavelets. Finally, the IDWT method fuses these subband images and generates high-resolution images. Deng G (2011) introduced a generalized unsharp masking (GUM) method, which enhances image sharpness by creating an exploratory data model as the framework. The GUM method can enhance the contrast and sharpness at the same time, eliminating the halo artifact. Nevertheless, the effect of preserving the edges is poor. Fu et al. (2015) proposed a probabilistic (PB) method of linear enhancement based on illumination and reflectance. Compared with the logarithmic domain, the linear domain model can better indicate the prior information. They use an alternating direction method of multipliers to effectively estimate the reflectance and illumination, resulting in pleasing results. However, the PB method cannot expand the dynamic range to enhance contrast.

This subsection provides an insight into the histogram equalization approach. Histogram equalization and its evolutionary approaches ignore the underwater optical imaging model, which can enhance the contrast; artifacts and noise are introduced. If some applications need to enhance the contrast of the underwater image, histogram equalization can be added to the UOIM-based method as post-processing. The next subsection is dedicated to color correction approaches and their merits and demerits.

3.2.2 Color correction approaches

Although histogram equalization approaches can effectively enhance contrast, these approaches cannot solve color cast. For instance, the white balance approaches in color spaces and the Retinex approach (Raihan et al., 2019) were proposed to keep the color constant.

1. White balance approaches

White balance is used to improve the color cast of the image. In water, the perception of color is related to depth, and a crucial problem is the blue-greenish effect that needs to be corrected. We compared existing partial white balance methods: MaxRGB (Land, 1977), gray world (Buchsbaum, 1980), shades of gray (Finlayson and Trezzi, 2004), gray edge (van de Weijer et al., 2007), weighted gray edge (Gijsenij et al., 2012), and automatic white balance (Weng et al., 2005). These methods aim at removing the undesired color shift due to the selective absorption caused by illumination or medium. Most of these methods make a specific assumption about the color of the light source. These methods achieve color constancy by dividing each color channel by the corresponding normalized light source intensity.

Among these approaches, the MaxRGB method (Land, 1977) assumes that the reflections from RGB channels are equal, selecting the maximum RGB values from different channels for the estimation of the light source; the gray world method (Buchsbaum, 1980) assumes that the average values of the average reflections of the light in natural scenes are fixed in most cases, using the average pixel values of the three channels to estimate the light color, and the fixed value is similar to "gray;" the shades of gray method (Finlayson and Trezzi, 2004) calculates the light value of each channel in the scenes by the Minkowski p-norm. When p=1, this method is a particular case of the gray world method; when p=∞, it can be seen as the MaxRGB method. The gray edge method (van de Weijer et al., 2007), which is the gray edge assumption, assumes that the average value of the differentials of the surface reflection coefficients in the scenes is achromatic. Based on the derivative structure of the images, this method achieves a color constant. The weighted gray edge method (Gijsenij et al., 2012) evaluates the performance of the constancy of edge colors using these different edge types. The automatic white balance method (Weng et al., 2005) examines the preferential white dots in the scenes using a dynamic threshold.

As depicted in Fig. 8, the gray world method (Buchsbaum, 1980) can effectively remove the bluish color cast. Due to the overcompensation of the red channel, the resulting images for this method present reddish artifacts. Although the white balance techniques are crucial in removing the color cast, these methods are not sufficient for solving the blurring and unsharp edge problem caused by inherent scattering.

2. Approaches in other color spaces

In the RGB color space, components of the three-color channels are closely connected. Thus, it is difficult to correct colors by modulating the three components. Some researchers have proposed methods for other color spaces, including HSI, HSV, and CIE-Lab (Tang C et al., 2019).

Torres-Méndez and Dudek (2005) used learning constraints to convert the problem of color restoration to energy minimization. This method uses the Markov random field (MRF) to describe the relatedness between color-distorted images and real-color underwater images. Using belief propagation, this method distributes the possible color information to the pixels in the color-distorted images. This method also uses abundant underwater scene data to examine the reliability. Some factors influence the color correction effects, such as inadequate reliable information as an input and statistical inconsistency of the images in the training set. Iqbal et al. (2007) proposed the integrated color model (ICM) based on underwater images that slid and stretch in the RGB color space and HSI color space. This method balances the image contrast and enhances the saturability and brightness of the images, optimizing the image color. Iqbal et al. (2010) proposed the unsupervised color correction method (UCM) to deal with the problems of low contrast and uneven color cast brought about by underwater scattering and absorption. This method reduces color cast by equalizing color values and enhances the images by contrast enhancement, stretching the red histogram to the right maximum value and stretching the blue histogram to the left minimum value. Finally, this method uses the saturability and brightness of the HSI color model to enhance contrast, using saturability to enhance color authenticity and correcting the brightness components to deal with the problem of light

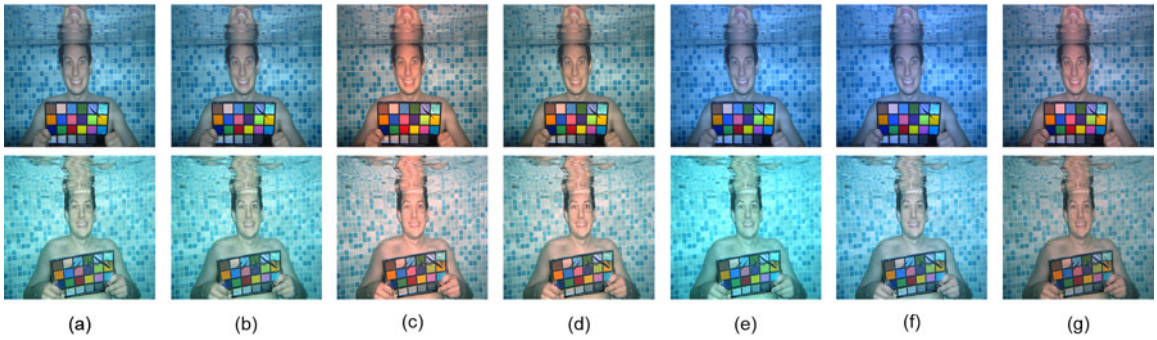

Fig. 8 Results of different white balance methods: (a) raw images; (b) MaxRGB (Land, 1977); (c) gray world (Buchsbaum, 1980); (d) shades of gray (Finlayson and Trezzi, 2004); (e) gray edge (van de Weijer et al., 2007); (f) weighted gray edge (Gijsenij et al., 2012); (g) automatic white balance (Weng et al., 2005)

References to color refer to the online version of this figure

intensity. However, the enhancement for some parts of the composed images is not well addressed, creating noise at the same time. Ghani and Isa (2014) introduced the composition of dual-intensity images and the Rayleigh-stretching method to enhance the quality of underwater images. This method applies the improved von Kries hypothesis, guaranteeing the rationality of the evaluation of gain coefficients. At the same time, this method uses the average value distributed by Rayleigh to stretch into two images of different intensities. However, some parts of the green channel are greatly enhanced, resulting in the dim restored images. Based on Iqbal's method, Ghani and Isa (2015a) redistributed the input images by combining the Rayleigh distribution function with the changes of ICM and UCM, further enhancing the image contrast and reducing over-enhancement, oversaturability, and noise. To deal with the issue of color cast, Ghani and Isa (2017) proposed the recursive adaptive histogram modification (RAHIM) method, which modifies the histogram according to Rayleigh distribution. In the HSV space, this method modifies the saturability and brightness of images to strengthen the natural attributes of the images, turning the images into the RGB space and obtaining the enhanced images.

In another interesting set of studies, Ghani et al. (2016) conducted work based on the Rayleigh distribution in the RGB and HSV color models to combine two images of different intensities. This method corrects the colors by selecting the average values to guarantee the appropriate gain factor values. As for deep-water images though, the enhancement is not significant. Based on Ghani et al. (2016), Azmi et al. (2019) proposed nature-based underwater image color enhancement through the fusion of a swarm-intelligence algorithm, which superimposes color cast neutralization, dual-intensity image fusion, and means equalization steps. This method can effectively solve the problem of bluish color cast. Based on the RGB and CIE-Lab color models, Huang DM et al. (2018) proposed the relative global histogram stretch (RGHS) method. Based on the images preprocessed using the gray world theory, this method adopts the adaptive histogram stretching in the RGB color model according to the distribution characteristics of the RGB channel and the selective decay of the light transmission in water. Finally, this method conducts linear and curve adaptive stretching optimization of the brightness L and components of colors a and b in the CIE-Lab color space retrospectively. The relative global histogram stretch method can improve the visual effect of images and restore useful information.

3. Retinex

The Retinex model simulates the perception mechanism of the human visual system, achieving color constancy, local contrast enhancement, dynamic range condensation, and others by estimating and eliminating the illumination in the scenes. It can be known from this model that the object colors perceived by human eyes are related to the reflection characteristics of the object surface, but the object colors are not related to the particular object illumination. In early research, this method was applied to image defogging (Wang YF et al., 2016). Because there exist similar circumstances in the underwater

environment, some researchers use this method to enhance the underwater image.

Joshi and Kamathe (2008) used the Retinex method to enhance underwater images. Compared with the enhanced images of foggy days, underwater image enhancement has some limitations. Fu et al. (2014) proposed a variational Retinex single underwater image enhancement method. The method converts underwater images into the Lab color space, decomposing the reflection rate and light by Retinex and the L component. This method uses bilateral filtering and trilateral filtering to process different colors under different restrictions, improving image colors, enhancing the brightness of the dark regions in the images, and enhancing edges and details. This method involves 4–6 iterations of the process, which has high time complexity. Alex and Supriya (2015) proposed an underwater image enhancement algorithm based on single-scale Retinex. This method converts images into the YCbCr color space, using the Gaussian function to conduct convolution processing while enhancing the Y and Cr components. The method has been shown to work except that the enhancement is uneven. Zhang S et al. (2017) proposed an underwater image enhancement method based on the expansion of the multi-scale Retinex. According to the characteristics of the three channels in the CIE-Lab color space, this method conducts bilateral filtering and trilateral filtering for the brightness channel L and the color components a and b, eliminating the incident light and restricting the halo artifact. Zhou et al. (2019b) proposed the Retinex-based Laplacian pyramid method. This method adds the Gamma correction illumination back to reflection to achieve color enhancement, and then detail enhancement is achieved by the Laplacian pyramid to process the reflection component. Finally, the detailed enhanced image and color corrected image are used to reconstruct a clear image.

Figs. 9b–9h show the comparison results produced by underwater image enhancement methods. They are effective non-physical methods. As shown in Fig. 9b, Iqbal's method (Iqbal et al., 2007) cannot improve the visual effect of overall images when the background has a bluish color cast. The yellowish resulting images are produced by Iqbal's method (Iqbal et al., 2010) when the histogram of the blue channel cannot be stretched effectively. Compared with Iqbal's method (Iqbal et al., 2007, 2010), Ghani's method (Ghani and Isa, 2014) successfully increases detailed information and reduces the noise. Because the underwater image has lower contrast than the natural image, the edge information is not obvious. Therefore, Fig. 9d shows a reddish appearance. Fig. 9e shows that Huang's method (Huang DM et al., 2018) presents better details, color saturation, and removes the noise. Pan's method (Pan et al., 2018) can remove color distortion and improve the clarity of underwater images. Yet, this method can enhance only part of the degraded images. Fu's method (Fu et al., 2014) and Zhou's method (Zhou et al., 2019b) can effectively improve global naturalness, because these methods are based on Retinex; they not only enhance details but also adjust illumination to match the human visual system. Zhou's method (Zhou et al., 2019b) can maintain the genuine color of the image.

3.2.3 Fusion-based approaches

Fusion-based approaches adopt the fusion strategy to fuse images with different image characteristics. Ancuti et al. (2012) enhanced the visual effect of underwater images and videos based on fusion. This method first obtains the contrast-enhanced image and fuses it with a color-corrected image, then defines the four fusion weights according to the holistic contrast, partial contrast, salience map, and exposure image of the two images, and finally fuses the fusion component diagram with the defined weight component diagram based on a multi-scale fusion strategy. This method can effectively solve the color cast of images and videos, enhancing contrast. However, as for different underwater environments, the weighting coefficient in the fusion process is hard to determine. Ghani and Isa (2015b) proposed a novel method which fuses the holistic and partial contrast to correct and enhance low-quality underwater images. This method can enhance the image contrast and improve image details at the same time. For images of low brightness, however, there would be color distortion. Li CY et al. (2017) proposed a fusion method based on color correction and underwater image defogging. This method uses the color prior to correct the underwater image color model, and then the improved image defogging methods to enhance the visual effect of the underwater images.

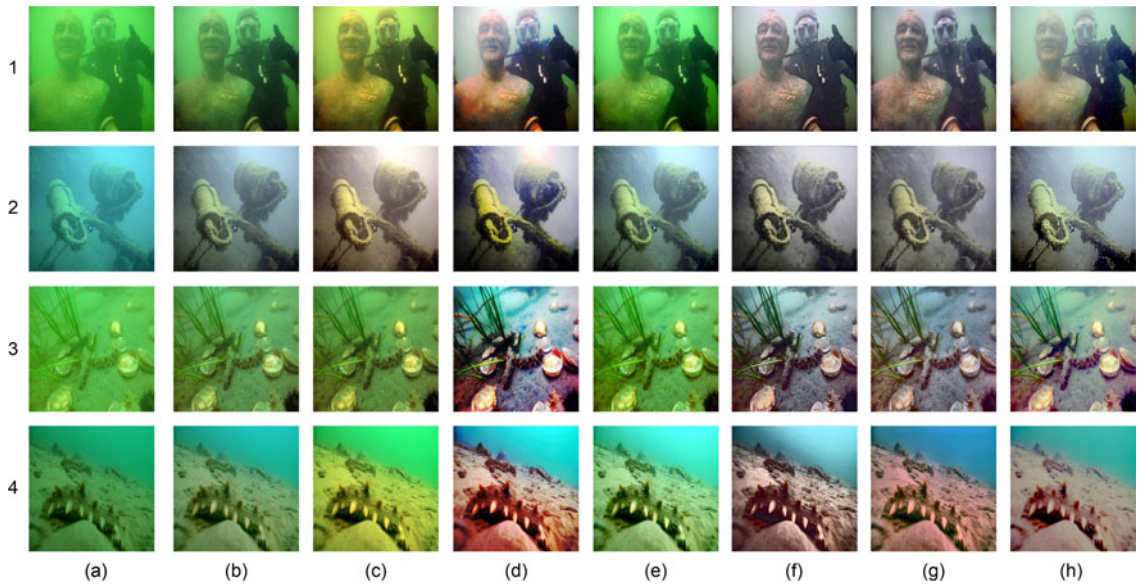

Fig. 9 Comparison of underwater image enhancement methods: (a) underwater raw images; (b–h) images obtained using Iqbal et al. (2007), Iqbal et al. (2010), Ghani and Isa (2014), Huang DM et al. (2018), Pan et al. (2018), Fu et al. (2014), and Zhou et al. (2019b)'s methods, respectively

Rows 1 and 2 are reprinted from the public data sets given by Li CY et al. (2019). References to color refer to the online version of this figure

Based on a variation of the study in 2012, Ancuti et al. (2018) proposed a novel method for color balance and underwater image enhancement. According to the underwater optical imaging principles, this method uses Gamma correction and sharpness to obtain two fusion weight images, using a multi-scale fusion strategy to fuse the two-weight maps and obtain the final enhanced image. This method reduces the over-enhancement and over-exposure, which can better process the dark regions of the image, enhancing the holistic contrast and edge clearness. Nevertheless, there is over-enhancement or insufficient enhancement in some parts of the fused image.

The underwater image enhancement method based on fusion, which uses the multi-scale fusion strategy, can effectively avoid the halo artifact caused by linear fusion, thus enhancing the images. This method ignores the imaging principles though, and thus there is over-enhancement or over-saturation in different areas.

The underwater image enhancement approach can more easily and quickly improve the visual effect of underwater images, but these methods neglect the underwater imaging model, which cannot comprehensively solve the problem of underwater image degeneration. The amplification of noise, color cast, and halo artifacts remain.

3.3 Approaches based on deep learning

Recently, deep learning technology has been extensively applied to underwater image defogging, and it can improve the quality of underwater images to some extent. Deep learning based methods can reduce errors caused by invalid priors by training a neural network to study the relationship between the image sets and relevant TMs (Wang KY et al., 2019). The underwater image enhancement methods based on deep learning can be classified into two main categories, methods based on CNNs (Ren et al., 2019) and methods based on GANs (Cai WW and Wei, 2020). The primary goal of CNN methods is to be loyal to the original underwater images, while the GAN methods are used to improve the perceived quality of images.

3.3.1 CNN-based approaches

CNN is composed of many network layers, including the input layer, hidden layer, and output layer. The hidden layer consists of the convolutional layer, pooling layer, and fully connected layer (Ren et al., 2020). CNN can provide great deformation modeling capability, but this method is applicable only to

certain underwater scenes, which are similar to the training set scenes, thus providing low applicability.

Cai BL et al. (2016) proposed a trainable end-to-end estimation network of the media TM, DehazeNet. This network takes the blurred images as input and outputs the medium TM, which is used to restore the defogged images through the atmospheric model. The network takes a deep structure based on CNN, which is designed to indicate the structured hypotheses during the defogging of the prior knowledge, resulting in a great defogging effect. Ding et al. (2017) used CNN to estimate the scene depth information of underwater white balance images after correction, and to estimate the TM. This method uses the average color values of the images after adjusting for the global BL. Perez et al. (2017) proposed an underwater image restoration method based on CNN, which restores the image quality by generating single images as the input images. This method examines the generalization ability of the neural network using images at different positions and of different characteristics. Wang Y et al. (2017) proposed an underwater image enhancement net based on CNN, which is called the UIE-net. This network is composed of two sub-networks to correct colors and defogging. This model is trained efficiently using a synthetic underwater image database. The convolutional layer is used to train and study the difference between the degraded underwater images and the clear images. It was determined that this model has good applicability through an ablation study. Pan et al. (2018) proposed de-scattering and enhancement using DehazeNet and HWD (DSDH). This method uses CNN to conduct end-to-end training of the estimated TM, using adaptive bilateral filtering to refine the TM. Then, this method uses white balance to eliminate the color difference, using the Laplacian pyramid to obtain the detail-enhanced and color-corrected images, and finally converts the output images into a hybrid domain of wavelet and directional filtering, eliminating noise, preserving edges, and improving the clearness of images. Li CY et al. (2020) proposed a CNN underwater image enhancement model, called UWCNN.

3.3.2 GAN-based approaches

Recently, GAN methods have been extensively applied to underwater image enhancement, showing great potential. A well-trained GAN-based method can recover the various underwater scenarios using paired data sets (Chen et al., 2019).

Zhu et al. (2017) used the cycle-consistent generative adversarial networks (CycleGAN) to generate approximately 4000 pairs of synthetic underwater images as the training data set for underwater images. Fabbri et al. (2018) adopted CycleGAN for restoration of underwater images, using the synthetic data set to train the GAN, and improving the underwater image quality based on an underwater generative adversarial network (UGAN). Kim T et al. (2017) proposed a model based on CycleGAN, which uses the relationship between domains, converting the images from one domain to another without training data or deeply matched circumstances, preserving the key attributes. Li J et al. (2018) proposed WaterGAN for restoration of underwater images. This network generates clean in-air images into turbid underwater images, constructing coupled data sets to train the neural network for enhancement of underwater images. WaterGAN consists of generator G and discriminator D. The discriminator is used to distinguish the real images from the synthetic images. The generator aims to generate images that would be identified as real images by the discriminator. This method is effective for the underwater images in the training samples, but it has limitations for real underwater images of different types. Chen et al. (2019) adopted the underwater imaging model to generate clear images from turbid underwater images, using coupled data sets to train the GAN for image enhancement. Li CY et al. (2018) proposed a weakly supervised color transfer method for underwater image color correction (UWGAN). This model does not need to train coupled underwater images, which allows taking underwater images at unknown positions. This model follows the path of CycleGAN, adopting the cycle structure, including the forward network and the back network. This model studies the mapping function between the source domain and the target domain, aiming to capture the unique characteristics of one image set and find out how to convert these characteristics into another image set. Inspired by GANs, Guo et al. (2020) proposed a multi-scale dense GAN for underwater image enhancement. This method introduces multi-scale, dense concatenation, and residual learning strategies to improve the visual effect of underwater images. The model cannot generate pleasing results. To increase the visual quality of the underwater image in real time, a GAN-based

restoration scheme was proposed by Chen et al. (2019). The scheme uses the single-shot network. It can preserve the image content and remove noise through a multibranch discriminator.

Compared with other underwater image enhancement methods, underwater image enhancement methods based on deep learning can achieve underwater image clearness. However, underwater image enhancement methods based on deep learning require paired image data sets to train the model, and obtaining enough paired images is difficult. These methods also have high requirements for hardware equipment. Thus, their applicability is limited.

4 Evaluation metrics

To evaluate the clarity of underwater images, researchers have designed a variety of image evaluation metrics. The major performance metrics are shown in Table 2, including: average gradient (AG) (He N et al., 2015), information entropy (IE) (He N et al., 2015), mean squared error (MSE) (He N et al., 2015), peak signal-to-noise ratio (PSNR) (He N et al., 2015), structural similarity (SSIM) (Wang Z and Bovik, 2006), rate of visible edges (e) (Hautière et al., 2008), saturation (σ) (Hautière et al., 2008), quality of contrast restoration ($\bar{r}$) (Hautière et al., 2008), patch-based contrast quality index (PCQI) (Wang SQ et al., 2015), underwater color image quality evaluation (UCIQE) (Yang M and Sowmya, 2015), and underwater image quality measure (UIQM) (Panetta et al., 2016).

The evaluation metrics for unambiguous underwater image methods can be classified into autonomous evaluation metrics and the human system of vision. There are no acknowledged criteria to evaluate the performances of underwater image processing objectively. Common metrics used for the evaluation of underwater image quality are PCQI, UCIQE, and UIQM. The elaboration of the evaluation metrics is as follows:

1. PCQI

PCQI is used to predict human perception of changes in contrast, calculating the average value, signal intensity, and signal structure in each patch, to compare the differences in contrast between images. Higher PCQI values indicate higher contrast.

Fig. 10 shows the PCQI metric to quantify the results of underwater restoration methods and underwater enhancement methods. Fig. 10a presents the PCQI values of the image restoration methods listed in Fig. 5. Due to the high contrast of restored images, the methods from Li CY et al. (2016) and Song et al. (2018) contribute to the highest PCQI value. In the resulting images processed by Li CY et al. (2016)'s method, three of four UIQM values show the highest value. For their method, 75% of the PCQI values are above average values. Hence, the methods of Li CY et al. (2016) can effectively increase the contrast of underwater images.

Fig. 10b presents the PCQI values of the image enhancement methods listed in Fig. 9. The methods of Iqbal et al. (2010) and Fu et al. (2014) show the highest PCQI values. The PCQI values from Fu et al. (2014)'s method are higher than the average values, so their method can effectively improve the visual results.

2. UCIQE

UCIQE is based on the linear combination of chroma, saturation, and contrast under the CIE-Lab model. It is the no-reference image quality evaluation metric. The larger value of UCIQE indicates higher image quality. c_1, c_2, and c_3 denote the weighting coefficients (c_1=0.4859, c_2=0.2745, c_3=0.2576).

Fig. 11 shows the UCIQE metric to quantify the results of the underwater restoration methods and underwater enhancement methods. Fig. 11a presents the UCIQE values of the image restoration methods listed in Fig. 5. Owing to the high contrast, saturation, and chroma of the restored images, the method of Li CY et al. (2016) demonstrates the highest UCIQE value. Compared to other methods, the one from Li CY et al. (2016) can produce visually pleasing results, though with fewer halos.

Fig. 11b presents the UCIQE values of the image enhancement methods listed in Fig. 9. Ghani and Isa (2014)'s method leads to the highest UCIQE values, which demonstrates that the enhancement results have higher contrast and saturation.

3. UIQM

UIQM uses a linear combination of three measures, which are the underwater image colorfulness measure (UICM), underwater image sharpness measure (UISM), and underwater image contrast measure (UIConM). The higher the UIQM value, the

Table 2 Objective evaluation metrics

Metric	Formula	Significance
AG	$\frac{1}{MN}\sum_{x=1}^{M}\sum_{y=1}^{N}\sqrt{\frac{1}{2}\left(\left[\frac{\partial F(x,y)}{\partial x}\right]^2+\left[\frac{\partial F(x,y)}{\partial y}\right]^2\right)}$, where M and N represent the sizes of the image	Higher AG reflects better image clarity
IE	$\sum_{i=0,p(i)\neq 0}^{255} p(i)\log\left(\frac{1}{p(i)}\right)$, where $p(i)$ (i=0, 1, …, 255) represents the probability distribution	Higher IE indicates more information of an image
MSE	$\frac{1}{MN}\sum_{i=0}^{M-1}\sum_{j=0}^{N-1}\left[I_1(i,j)-I_2(i,j)\right]^2$, where I_1 is the original image and I_2 is the defogging image	Lower MSE represents better recovery
PSNR	$10\lg\left(\max\left(\frac{(I_1,I_2)^2}{\mathrm{MSE}}\right)\right)$, (I_1, I_2)=255	Higher PSNR represents better quality of the restored image
SSIM	$\frac{2\mu_x\mu_y+C_1}{\mu_x^2+\mu_y^2+C_1}\frac{2\sigma_x\sigma_y+C_2}{\sigma_x^2+\sigma_y^2+C_2}$, where μ_x and μ_y are means, σ_x and σ_y are standard deviations, and C_1 and C_2 are constants	Higher SSIM means more restoration information of the raw image
e	$(n_r-n_0)/n_0$, where n_0 and n_r denote the numbers in the sets of visible edges in I_0 and I_r, respectively	Higher e shows more restored edges
σ	$n_s/(MN)$, where n_s represents the number of saturated pixels	Lower σ shows better contrast
$\bar{\gamma}$	$\exp\left(\frac{1}{n}\sum_{p_i\in\Omega_y}\log\gamma_i\right)$	Higher $\bar{\gamma}$ shows better contrast restoration
PCQI	$\frac{1}{M}\sum_{i=1}^{M}q_i(x_i,y_i)q_c(x_i,y_i)q_s(x_i,y_i)$, where M indicates the total number of patches in the image, $q_i(x_i, y_i)$ is the mean intensity, $q_c(x_i, y_i)$ is used to determine the structural distortion, and $q_s(x_i, y_i)$ represents the changes in contrast	Higher PCQI represents better contrast of the image
UCIQE	$c_1\sigma_c+c_2\mathrm{con}_l+c_3\mu_s$, where σ_c, con_l, and μ_s indicate the standard deviation of chroma, the contrast in brightness, and the average value of saturation, respectively, and c_1, c_2, and c_3 denote the weighting coefficients	Higher UCIQE means better image quality in chroma, saturation, and contrast
UIQM	c_1UICM+c_2UISM+c_3UIConM, where c_1, c_2, and c_3 denote the weighting coefficients	Higher UIQM means better comprehensive performance in color, contrast, and sharpness

AG: average gradient; IE: information entropy; MSE: mean squared error; PSNR: peak signal-to-noise ratio; SSIM: structural similarity; e: rate of visible edges; σ: saturation; $\bar{\gamma}$: quality of contrast restoration; PCQI: patch-based contrast quality index; UCIQE: underwater color image quality evaluation; UIQM: under-water image quality measure

better the visual effect of the image. The selection of three coefficients is determined by the application scene: c_1 is used to adjust underwater image colors; c_2 is used to enhance clearness of the underwater image; c_3 is used to enhance the image contrast of the underwater image (i.e., c_1=0.0282, c_2=0.2953, c_3=3.5753).

Fig. 12 shows the UIQM metric to quantify the results of the underwater restoration methods and underwater enhancement methods. Fig. 12a presents the UIQM values of the image restoration methods listed in Fig. 5. The methods from Peng et al. (2015), Li CY et al. (2016), and Peng and Cosman (2017) manifest the highest UIQM values, due to the high contrast sharpness of the restored images. In the resulting images processed by Li CY et al. (2016)'s method, two of the four UIQM values show the highest value. One of the four has the highest value, after processing the results with the methods from Peng et al. (2015) and Peng and Cosman (2017). Although the UIQM value of the image processed by Peng et al. (2015)'s method is higher than those of other methods, there is a greenish color cast. For

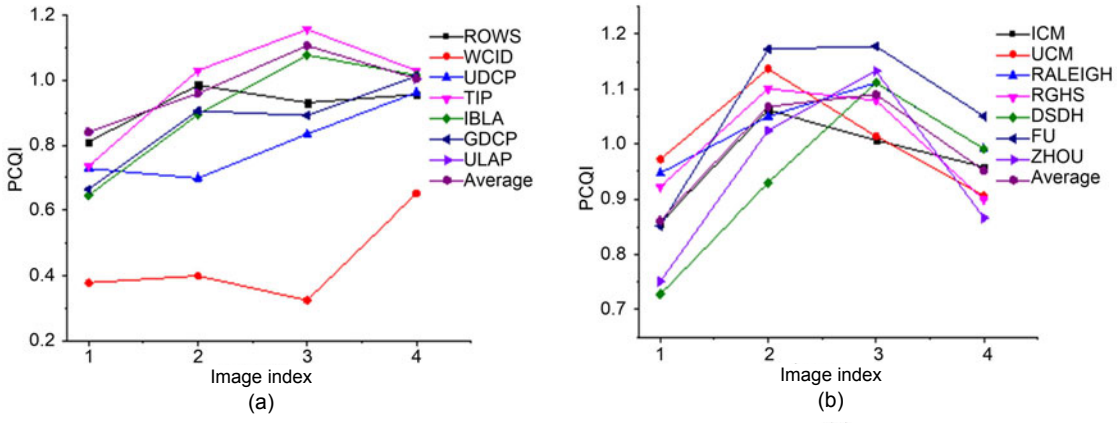

Fig. 10 The PCQI values of the compared methods: (a) underwater image restoration methods in Fig. 5; (b) underwater image enhancement methods in Fig. 9

Underwater image restoration methods: ROWS (Chao and Wang, 2010); WCID (Chiang and Chen, 2012); UDCP (Drews et al., 2013); TIP (Li CY et al., 2016); IBLA (Peng et al., 2015); GDCP (Peng and Cosman, 2017); ULAP (Song et al., 2018)

Underwater image enhancement methods: ICM (Iqbal et al., 2007); UCM (Iqbal et al., 2010); RALEIGH (Ghani and Isa, 2014); RGHS (Huang DM et al., 2018); DSDH (Pan et al., 2018); FU (Fu et al., 2014); ZHOU (Zhou et al., 2019b)

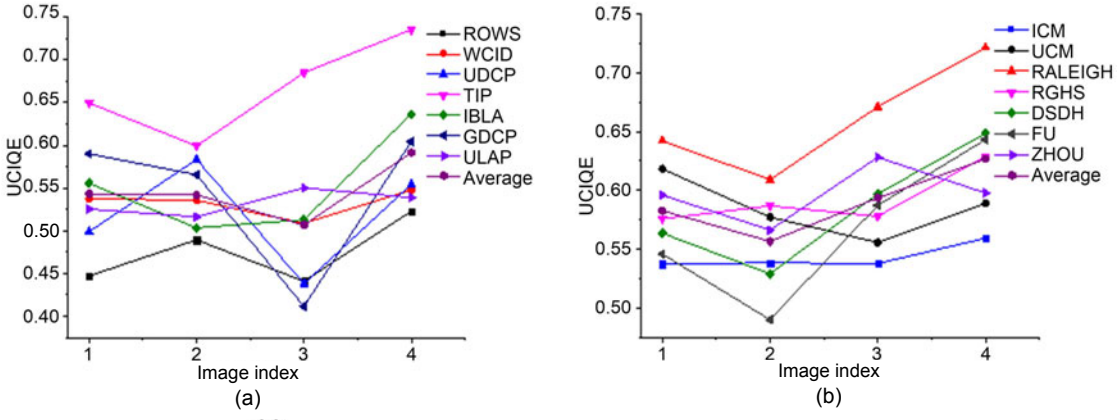

Fig. 11 The UCIQE values of the compared methods: (a) underwater image restoration methods in Fig. 5; (b) underwater image enhancement methods in Fig. 9

Underwater image restoration methods: ROWS (Chao and Wang, 2010); WCID (Chiang and Chen, 2012); UDCP (Drews et al., 2013); TIP (Li CY et al., 2016); IBLA (Peng et al., 2015); GDCP (Peng and Cosman, 2017); ULAP (Song et al., 2018)

Underwater image enhancement methods: ICM (Iqbal et al., 2007); UCM (Iqbal et al., 2010); RALEIGH (Ghani and Isa, 2014); RGHS (Huang DM et al., 2018); DSDH (Pan et al., 2018); FU (Fu et al., 2014); ZHOU (Zhou et al., 2019b)

Li CY et al. (2016)'s method, 75% of the UIQM values are above the average values. Thus, the method from Li CY et al. (2016) can effectively unveil more details and improve the contrast for underwater scenes.

Fig. 12b presents the UIQM values of the image enhancement methods listed in Fig. 9. Methods from Ghani and Isa (2014) and Fu et al. (2014) achieve the highest UIQM values, indicating that enhanced results have higher contrast and sharpness. The UIQM values from Ghani and Isa (2014) are higher than the average values, so this method can effectively improve image sharpness and color.

The contrast enhancement method proposed by Li CY et al. (2016) can produce two versions of enhanced output: one has relatively genuine color and natural appearance, and the other has higher contrast and more details. The two versions are fused to obtain higher contrast and sharpness, so it has higher PCQI, UCIQE, and UIQM values.

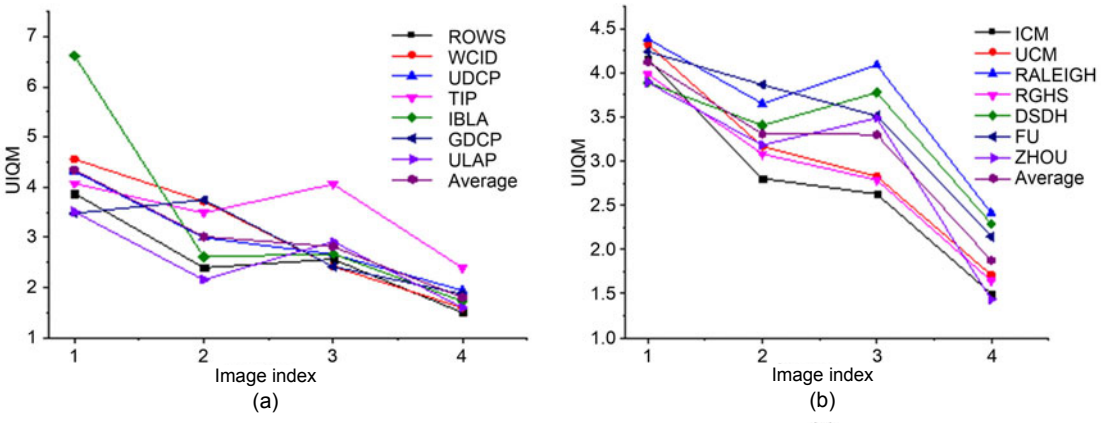

Fig. 12 The UIQM values of the compared methods: (a) underwater image restoration methods in Fig. 5; (b) underwater image enhancement methods in Fig. 9

Underwater image restoration methods: ROWS (Chao and Wang, 2010); WCID (Chiang and Chen, 2012); UDCP (Drews et al., 2013); TIP (Li CY et al., 2016); IBLA (Peng et al., 2015); GDCP (Peng and Cosman, 2017); ULAP (Song et al., 2018)

Underwater image enhancement methods: ICM (Iqbal et al., 2007); UCM (Iqbal et al., 2010); RALEIGH (Ghani and Isa, 2014); RGHS (Huang DM et al., 2018); DSDH (Pan et al., 2018); FU (Fu et al., 2014); ZHOU (Zhou et al., 2019b)

5 Conclusions and future research directions

In this paper we analyzed the reasons for the degeneration of underwater images, including absorption, scattering, noise, and halo. We classified, compared, and evaluated various image defogging approaches. Although not all classifications are covered, we have used several methods for each category to cover the field of underwater image defogging. These approaches have been divided into three categories, namely underwater image restoration approaches, underwater image enhancement approaches, and approaches based on deep learning. Lastly, we introduced a system for underwater image quality evaluation. Although unambiguous approaches in underwater imaging have made some progress, there still exist some problems to be solved.

In future research on underwater image enhancement and restoration, researchers may carry out work from the following perspectives:

1. Improve the robustness and adaptivity of the algorithms. The ideal methods should be adjusted according to different underwater application scenes and different types of degenerated images, and not be restricted by external conditions.

2. Decrease the complexity of methods and improve the processing results. To fulfill the demands of practical applications, the proposed methods should include instantaneity. At present, some underwater image restoration methods based on physical models and underwater image enhancement methods based on deep learning require considerable processing time; at the same time, the processing results should be further improved to solve problems of color cast, blurring of details, etc.

3. Most of the current underwater image enhancement methods focus on solving only one kind of problem. A comprehensive solution that can effectively solve the common problems of underwater images such as color cast, low contrast, noise, and blurring of details is required.

4. Most of the underwater image enhancement methods based on deep learning focus on the structural improvement of the current defogging networks. There are no network structures or loss functions designed especially for underwater images, which leads to unstable enhancement results. In most cases, deep learning methods fall behind advanced traditional methods (Anwar and Li, 2020).

5. Establish a standard system for evaluation of underwater image quality and data sets of underwater images. Currently, Li CY et al. (2019) have established standard public underwater data sets. As for machine learning, real data sets include limited scene information and numbers of scenes. At present, most of the training sets are synthesized artificially.

6. Underwater video processing technologies need further improvement. Most of the current

methods are used to process a single underwater image, and there are fewer underwater video processing technologies. As a crucial technology in the visual system, current processing methods focus mostly on hardware (examined cameras), and there are no effective underwater video processing technologies. The study of underwater video processing technologies should focus on instantaneity, guaranteeing satisfying defogging effects.

7. As a hot research field in recent years, text-to-image synthesis generates an image with content consistent with a given text description, which can be migrated to defogged underwater images to generate underwater images with strong contrast, rich details, and constant color (Yuan and Peng, 2018, 2020; Yin et al., 2019).

Contributors

Jing-chun ZHOU conceived the idea and drafted the paper. De-huan ZHANG carried out the experiments. Wei-shi ZHANG revised the paper and provided technical guidance. Jing-chun ZHOU and De-huan ZHANG revised and finalized the paper.

Compliance with ethics guidelines

Jing-chun ZHOU, De-huan ZHANG, and Wei-shi ZHANG declare that they have no conflict of interest.

References

Abu A, Diamant R, 2019. Unsupervised local spatial mixture segmentation of underwater objects in sonar images. *IEEE J Ocean Eng*, 44(4):1179-1197. https://doi.org/10.1109/JOE.2018.2863961

Alex RSM, Supriya MH, 2015. Underwater image enhancement using single scale retinex on a reconfigurable hardware. Int Symp on Ocean Electronics, p.1-5. https://doi.org/10.1109/SYMPOL.2015.7581166

Amer KO, Elbouz M, Alfalou A, 2019. Enhancing underwater optical imaging by using a low-pass polarization filter. *Opt Expr*, 27(2):621-643. https://doi.org/10.1364/OE.27.000621

Ancuti C, Ancuti CO, Haber T, et al., 2012. Enhancing underwater images and videos by fusion. IEEE Conf on Computer Vision and Pattern Recognition, p.81-88. https://doi.org/10.1109/CVPR.2012.6247661

Ancuti CO, Ancuti C, de Vleeschouwer C, et al., 2018. Color balance and fusion for underwater image enhancement. *IEEE Trans Image Process*, 27(1):379-393. https://doi.org/10.1109/TIP.2017.2759252

Anwar S, Li CY, 2020. Diving deeper into underwater image enhancement: a survey. *Signal Process Image Commun*, 89:115978. https://doi.org/10.1016/j.image.2020.115978

Azmi KZM, Ghani ASA, Yusof ZM, et al., 2019. Natural-based underwater image color enhancement through fusion of swarm-intelligence algorithm. *Appl Soft Comput*, 85:105810. https://doi.org/10.1016/j.asoc.2019.105810

Bai L, Zhang W, Pan X, et al., 2020. Underwater image enhancement based on global and local equalization of histogram and dual-image multi-scale fusion. *IEEE Access*, 8:128973-128990. https://10.1109/ACCESS.2020.3009161

Buchsbaum G, 1980. A spatial processor model for object colour perception. *J Franklin Inst*, 310(1):1-26. https://doi.org/10.1016/0016-0032(80)90058-7

Cai BL, Xu XM, Jia K, et al., 2016. DehazeNet: an end-to-end system for single image haze removal. *IEEE Trans Image Process*, 25(11):5187-5198. https://doi.org/10.1109/TIP.2016.2598681

Cai WW, Wei ZG, 2020. PiiGAN: generative adversarial networks for pluralistic image inpainting. *IEEE Access*, 8:48451-48463. https://doi.org/10.1109/ACCESS.2020.2979348

Carlevaris-Bianco N, Mohan A, Eustice RM, 2010. Initial results in underwater single image dehazing. OCEANS 2010 MTS/IEEE SEATTLE, p.1-8. https://doi.org/10.1109/OCEANS.2010.5664428

Chang YK, Jung CL, Ke P, et al., 2018. Automatic contrast-limited adaptive histogram equalization with dual Gamma correction. *IEEE Access*, 6:11782-11792. https://doi.org/10.1109/ACCESS.2018.2797872

Chao L, Wang M, 2010. Removal of water scattering. Proc 2nd Int Conf on Computer Engineering and Technology, p.35-39. https://doi.org/10.1109/ICCET.2010.5485339

Chen XY, Yu JZ, Kong SH, et al., 2019. Towards real-time advancement of underwater visual quality with GAN. *IEEE Trans Ind Electron*, 66(12):9350-9359. https://doi.org/10.1109/TIE.2019.2893840

Chiang JY, Chen YC, 2012. Underwater image enhancement by wavelength compensation and dehazing. *IEEE Trans Image Process*, 21(4):1756-1769. https://doi.org/10.1109/TIP.2011.2179666

Dai CG, Lin MX, Wu XJ, et al., 2020. Single underwater image restoration by decomposing curves of attenuating color. *Opt Laser Technol*, 123:105947. https://doi.org/10.1016/j.optlastec.2019.105947

Demirel H, Anbarjafari G, 2011. IMAGE resolution enhancement by using discrete and stationary wavelet decomposition. *IEEE Trans Image Process*, 20(5):1458-1460. https://doi.org/10.1109/TIP.2010.2087767

Deng G, 2011. A generalized unsharp masking algorithm. *IEEE Trans Image Process*, 20(5):1249-1261. https://doi.org/10.1109/TIP.2010.2092441

Deng XY, Wang HG, Liu X, 2019. Underwater image enhancement based on removing light source color and dehazing. *IEEE Access*, 7:114297-114309. https://doi.org/10.1109/ACCESS.2019.2936029

Ding XY, Wang YF, Zhang J, et al., 2017. Underwater image dehaze using scene depth estimation with adaptive color

correction. OCEANS Aberdeen, p.1-5. https://doi.org/10.1109/OCEANSE.2017.8084665

Drews PJr, Do Nascimento E, Moraes F, et al., 2013. Transmission estimation in underwater single images. Proc IEEE Int Conf on Computer Vision Workshops, p.825-830. https://doi.org/10.1109/ICCVW.2013.113

Duntley SQ, 1963. Light in the sea. *J Opt Soc Am*, 53(2): 214-233. https://doi.org/10.1364/JOSA.53.000214

Fabbri C, Islam MJ, Sattar J, 2018. Enhancing underwater imagery using generative adversarial networks. IEEE Int Conf on Robotics and Automation, p.7159-7165. https://doi.org/10.1109/ICRA.2018.8460552

Finlayson GD, Trezzi E, 2004. Shades of gray and colour constancy. Proc 12th Color Imaging Conf, p.37-41.

Fu XY, Zhuang PX, Huang Y, et al., 2014. A retinex-based enhancing approach for single underwater image. IEEE Int Conf on Image Processing, p.4572-4576. https://doi.org/10.1109/ICIP.2014.7025927

Fu XY, Liao YH, Zeng DL, et al., 2015. A probabilistic method for image enhancement with simultaneous illumination and reflectance estimation. *IEEE Trans Image Process*, 24(12):4965-4977. https://doi.org/10.1109/TIP.2015.2474701

Galdran A, Pardo D, Picón A, et al., 2015. Automatic red-channel underwater image restoration. *J Vis Commun Image Represent*, 26:132-145. https://doi.org/10.1016/j.jvcir.2014.11.006

Gao SB, Zhang M, Zhao Q, et al., 2019. Underwater image enhancement using adaptive retinal mechanisms. *IEEE Trans Image Process*, 28(11):5580-5595. https://doi.org/10.1109/TIP.2019.2919947

Ghani ASA, Isa NAM, 2014. Underwater image quality enhancement through composition of dual-intensity images and Rayleigh-stretching. *SpringerPlus*, 3(1):757. https://doi.org/10.1186/2193-1801-3-757

Ghani ASA, Isa NAM, 2015a. Underwater image quality enhancement through integrated color model with Rayleigh distribution. *Appl Soft Comput*, 27:219-230. https://doi.org/10.1016/j.asoc.2014.11.020

Ghani ASA, Isa NAM, 2015b. Enhancement of low quality underwater image through integrated global and local contrast correction. *Appl Soft Comput*, 37:332-344. https://doi.org/10.1016/j.asoc.2015.08.033

Ghani ASA, Isa NAM, 2017. Automatic system for improving underwater image contrast and color through recursive adaptive histogram modification. *Comput Electron Agric*, 141:181-195. https://doi.org/10.1016/j.compag.2017.07.021

Ghani ASA, Aris RSNAR, Zain MLM, 2016. Unsupervised contrast correction for underwater image quality enhancement through integrated-intensity stretched-Rayleigh histograms. *J Telecomm Electron Comput Eng*, 8(3):1-7.

Giakos GC, 2004. Active backscattered optical polarimetric imaging of scattered targets. Proc 21st IEEE Instrumentation and Measurement Technology Conf, p.430-432. https://doi.org/10.1109/IMTC.2004.1351080

Gijsenij A, Gevers T, van de Weijer J, 2012. Improving color constancy by photometric edge weighting. *IEEE Trans Patt Anal Mach Intell*, 34(5):918-929. https://doi.org/10.1109/TPAMI.2011.197

Guo YC, Li HY, Zhuang PX, 2020. Underwater image enhancement using a multiscale dense generative adversarial network. *IEEE J Ocean Eng*, 45(3):862-870. https://doi.org/10.1109/JOE.2019.2911447

Han M, Lyu ZY, Qiu T, et al., 2020. A review on intelligence dehazing and color restoration for underwater images. *IEEE Trans Syst Man Cybern Syst*, 50(5):1820-1832. https://doi.org/10.1109/TSMC.2017.2788902

Han PL, Liu F, Zhang G, et al., 2018. Multi-scale analysis method of underwater polarization imaging. *Acta Phys Sin*, 67(5):054202 (in Chinese). https://doi.org/10.7498/aps.67.20172009

Hautière N, Tarel JP, Aubert D, et al., 2008. Blind contrast enhancement assessment by gradient ratioing at visible edges. *Image Anal Stereol*, 27(2):87-95. https://doi.org/10.5566/ias.v27.p87-95

He KM, Sun J, Tang XO, 2009. Single image haze removal using dark channel prior. Proc IEEE Computer Society Conf on Computer Vision and Pattern Recognition, p.1956-1963. https://doi.org/10.1109/CVPR.2009.5206515

He N, Wang JB, Zhang LL, et al., 2015. An improved fractional-order differentiation model for image denoising. *Signal Process*, 112:180-188. https://doi.org/10.1016/j.sigpro.2014.08.025

Hou GJ, Pan ZK, Wang GD, et al., 2019. An efficient nonlocal variational method with application to underwater image restoration. *Neurocomputing*, 369:106-121. https://doi.org/10.1016/j.neucom.2019.08.041

Hu HF, Zhao L, Huang BJ, et al., 2017. Enhancing visibility of polarimetric underwater image by transmittance correction. *IEEE Photon J*, 9(3):6802310. https://doi.org/10.1109/JPHOT.2017.2698000

Hu HF, Zhao L, Li XB, et al., 2018. Underwater image recovery under the nonuniform optical field based on polarimetric imaging. *IEEE Photon J*, 10(1):6900309. https://doi.org/10.1109/JPHOT.2018.2791517

Huang BJ, Liu TG, Hu HF, et al., 2016. Underwater image recovery considering polarization effects of objects. *Opt Expr*, 24(9):9826-9838. https://doi.org/10.1364/OE.24.009826

Huang DM, Wang Y, Song W, et al., 2018. Shallow-water image enhancement using relative global histogram stretching based on adaptive parameter acquisition. Proc 24th Int Conf on Multimedia Modeling, p.453-465. https://doi.org/10.1007/978-3-319-73603-7_37

Hummel R, 1977. Image enhancement by histogram transformation. *Comput Graph Image Process*, 6(2):184-195. https://doi.org/10.1016/S0146-664X(77)80011-7

Iqbal K, Salam RA, Osman A, et al., 2007. Underwater image enhancement using an integrated colour model. *IAENG*

Int J Comput Sci, 34:2.

Iqbal K, Odetayo M, James A, et al., 2010. Enhancing the low quality images using unsupervised colour correction method. IEEE Int Conf on Systems, Man and Cybernetics, p.1703-1709. https://doi.org/10.1109/ICSMC.2010.5642311

Jaffe JS, 1990. Computer modeling and the design of optimal underwater imaging systems. *IEEE J Ocean Eng*, 15(2): 101-111. https://doi.org/10.1109/48.50695

Joshi KR, Kamathe RS, 2008. Quantification of retinex in enhancement of weather degraded images. Int Conf on Audio, Language and Image Processing, p.1229-1233. https://doi.org/10.1109/ICALIP.2008.4590120

Kapoor R, Gupta R, Son LH, et al., 2019. Fog removal in images using improved dark channel prior and contrast limited adaptive histogram equalization. *Multim Tools Appl*, 78(16):23281-23307. https://doi.org/10.1007/s11042-019-7574-8

Kim T, Cha M, Kim H, et al., 2017. Learning to discover cross-domain relations with generative adversarial networks. Proc 34th Int Conf on Machine Learning, p.1857-1865.

Kim TK, Paik JK, Kang BS, 1998. Contrast enhancement system using spatially adaptive histogram equalization with temporal filtering. *IEEE Trans Consum Electron*, 44(1):82-87. https://doi.org/10.1109/30.663733

Kim YT, 1997. Contrast enhancement using brightness preserving bi-histogram equalization. *IEEE Trans Consum Electron*, 43(1):1-8. https://doi.org/10.1109/30.580378

Land EH, 1977. The retinex theory of color vision. *Sci Am*, 237(6):108-128. https://doi.org/10.1038/scientificamerican1277-108

Lee Y, Gibson KB, Lee Z, et al., 2014. Stereo image defogging. Proc IEEE Int Conf on Image Processing, p.5427-5431. https://doi.org/10.1109/ICIP.2014.7026098

Li CY, Guo JC, Cong RM, et al., 2016. Underwater image enhancement by dehazing with minimum information loss and histogram distribution prior. *IEEE Trans Image Process*, 25(12):5664-5677. https://doi.org/10.1109/TIP.2016.2612882

Li CY, Guo JC, Guo CL, et al., 2017. A hybrid method for underwater image correction. *Patt Recogn Lett*, 94:62-67. https://doi.org/10.1016/j.patrec.2017.05.023

Li CY, Guo JC, Guo CL, 2018. Emerging from water: underwater image color correction based on weakly supervised color transfer. *IEEE Signal Process Lett*, 25(3):323-327. https://doi.org/10.1109/LSP.2018.2792050

Li CY, Guo CL, Ren WQ, et al., 2019. An underwater image enhancement benchmark dataset and beyond. *IEEE Trans Image Process*, 29:4376-4389. https://doi.org/10.1109/TIP.2019.2955241

Li CY, Anwar S, Porikli F, 2020. Underwater scene prior inspired deep underwater image and video enhancement. *Patt Recogn*, 98:107038. https://doi.org/10.1016/j.patcog.2019.107038

Li J, Skinner KA, Eustice RM, et al., 2018. WaterGAN: unsupervised generative network to enable real-time color correction of monocular underwater images. *IEEE Robot Autom Lett*, 3(1):387-394. https://doi.org/10.1109/LRA.2017.2730363

Li YJ, Lu HM, Li KC, et al., 2018. Non-uniform de-scattering and de-blurring of underwater images. *Mob Netw Appl*, 23(2):352-362. https://doi.org/10.1007/s11036-017-0933-7

Liu F, Wei Y, Han PL, et al., 2019. Polarization-based exploration for clear underwater vision in natural illumination. *Opt Expr*, 27(3):3629-3641. https://doi.org/10.1364/OE.27.003629

Liu P, Wang GY, Qi H, et al., 2019. Underwater image enhancement with a deep residual framework. *IEEE Access*, 7:94614-94629. https://doi.org/10.1109/ACCESS.2019.2928976

Liu TG, Guan ZJ, Li XB, et al., 2020. Polarimetric underwater image recovery for color image with crosstalk compensation. *Opt Lasers Eng*, 124:105833. https://doi.org/10.1016/j.optlaseng.2019.105833

Mangeruga M, Cozza M, Bruno F, 2018. Evaluation of underwater image enhancement algorithms under different environmental conditions. *J Mar Sci Eng*, 6(1):10. https://doi.org/10.3390/jmse6010010

Marques TP, Albu AB, Hoeberechts M, 2019. A contrast-guided approach for the enhancement of low-lighting underwater images. *J Imag*, 5(10):79. https://doi.org/10.3390/jimaging5100079

McGlamery BL, 1980. A computer model for underwater camera systems. Proc SPIE, Ocean Optics VI, 0208:221-231. https://doi.org/10.1117/12.958279

Nomura K, Sugimura D, Hamamoto T, 2018. Underwater image color correction using exposure-bracketing imaging. *IEEE Signal Process Lett*, 25(6):893-897. https://doi.org/10.1109/LSP.2018.2831630

Pan PW, Yuan F, Cheng E, 2018. Underwater image de-scattering and enhancing using DehazeNet and HWD. *J Mar Sci Technol*, 26(4):531-540. https://doi.org/10.6119/JMST.201808_26(4).0006

Pan PW, Yuan F, Cheng E, 2019. De-scattering and edge-enhancement algorithms for underwater image restoration. *Front Inform Technol Electron Eng*, 20(6):862-871. https://doi.org/10.1631/FITEE.1700744

Panetta K, Gao C, Agaian S, 2016. Human-visual-system-inspired underwater image quality measures. *IEEE J Ocean Eng*, 41(3):541-551. https://doi.org/10.1109/JOE.2015.2469915

Peng YT, Cosman PC, 2017. Underwater image restoration based on image blurriness and light absorption. *IEEE Trans Image Process*, 26(4):1579-1594. https://doi.org/10.1109/TIP.2017.2663846

Peng YT, Zhao XY, Cosman PC, 2015. Single underwater image enhancement using depth estimation based on blurriness. IEEE Int Conf on Image Processing, p.4952-4956. https://doi.org/10.1109/ICIP.2015.7351749

Peng YT, Cao KM, Cosman PC, 2018. Generalization of the dark channel prior for single image restoration. *IEEE Trans Image Process*, 27(6):2856-2868. https://doi.org/10.1109/TIP.2018.2813092

Perez J, Attanasio AC, Nechyporenko N, et al., 2017. A deep learning approach for underwater image enhancement. Int Work-Conf on the Interplay Between Natural and Artificial Computation, p.183-192. https://doi.org/10.1007/978-3-319-59773-7_19

Pizer SM, Amburn EP, Austin JD, et al., 1987. Adaptive histogram equalization and its variations. *Comput Vis Graph Image Process*, 39(3):355-368. https://doi.org/10.1016/S0734-189X(87)80186-X

Raihan AJ, Abas PE, de Silva LC, 2019. Review of underwater image restoration algorithms. *IET Image Process*, 13(10): 1587-1596. https://doi.org/10.1049/iet-ipr.2019.0117

Ren WQ, Liu SF, Ma L, et al., 2019. Low-light image enhancement via a deep hybrid network. *IEEE Trans Image Process*, 28(9):4364-4375. https://doi.org/10.1109/TIP.2019.2910412

Ren WQ, Pan JS, Zhang H, et al., 2020. Single image dehazing via multi-scale convolutional neural networks with holistic edges. *Int J Comput Vis*, 128(1):240-259. https://doi.org/10.1007/s11263-019-01235-8

Reza AM, 2004. Realization of the contrast limited adaptive histogram equalization (CLAHE) for real-time image enhancement. *J VLSI Signal Process Syst Signal Image Video Technol*, 38(1):35-44. https://doi.org/10.1023/B:VLSI.0000028532.53893.82

Roser M, Dunbabin M, Geiger A, 2014. Simultaneous underwater visibility assessment, enhancement and improved stereo. IEEE Int Conf on Robotics and Automation, p.3840-3847. https://doi.org/10.1109/ICRA.2014.6907416

Schechner YY, Averbuch Y, 2007. Regularized image recovery in scattering media. *IEEE Trans Patt Anal Mach Intell*, 29(9):1655-1660. https://doi.org/10.1109/TPAMI.2007.1141

Schechner YY, Karpel N, 2005. Recovery of underwater visibility and structure by polarization analysis. *IEEE J Ocean Eng*, 30(3):570-587. https://doi.org/10.1109/JOE.2005.850871

Schechner YY, Narasimhan SG, Nayar SK, 2001. Instant dehazing of images using polarization. Proc IEEE Computer Society Conf on Computer Vision and Pattern Recognition, p.325-332. https://doi.org/10.1109/CVPR.2001.990493

Schechner YY, Narasimhan SG, Nayar SK, 2003. Polarization-based vision through haze. *Appl Opt*, 42(3):511-525. https://doi.org/10.1364/AO.42.000511

Singh D, Kumar V, 2019. A comprehensive review of computational dehazing techniques. *Arch Comput Methods Eng*, 26(5):1395-1413. https://doi.org/10.1007/s11831-018-9294-z

Song W, Wang Y, Huang DM, et al., 2018. A rapid scene depth estimation model based on underwater light attenuation prior for underwater image restoration. Proc 19th Pacific-Rim Conf on Multimedia on Advances in Multimedia Information Processing, p.678-688. https://doi.org/10.1007/978-3-030-00776-8_62

Tang C, von Lukas UF, Vahl M, et al., 2019. Efficient underwater image and video enhancement based on retinex. *Signal Image Video Process*, 13(5):1011-1018. https://doi.org/10.1007/s11760-019-01439-y

Tang JR, Isa NAM, 2017. Bi-histogram equalization using modified histogram bins. *Appl Soft Comput*, 55:31-43. https://doi.org/10.1016/j.asoc.2017.01.053

Tian Y, Liu B, Su XY, et al., 2019. Underwater imaging based on LF and polarization. *IEEE Photon J*, 11(1):6500309. https://doi.org/10.1109/JPHOT.2018.2890286

Torres-Méndez LA, Dudek G. 2005. Color correction of underwater images for aquatic robot inspection. Proc 5th Int Workshop on Energy Minimization Methods in Computer Vision and Pattern Recognition, p.60-73. https://doi.org/10.1007/11585978_5

Treibitz T, Schechner YY, 2006. Instant 3Descatter. Proc IEEE Computer Society Conf on Computer Vision and Pattern Recognition, p.1861-1868. https://doi.org/10.1109/CVPR.2006.155

Treibitz T, Schechner YY, 2009. Active polarization descattering. *IEEE Trans Patt Anal Mach Intell*, 31(3):385-399. https://doi.org/10.1109/TPAMI.2008.85

Treibitz T, Schechner YY, 2012. Turbid scene enhancement using multi-directional illumination fusion. *IEEE Trans Image Process*, 21(11):4662-4667. https://doi.org/10.1109/TIP.2012.2208978

van de Weijer J, Gevers T, Gijsenij A, 2007. Edge-based color constancy. *IEEE Trans Image Process*, 16(9):2207-2214. https://doi.org/10.1109/TIP.2007.901808

Wang KY, Hu Y, Chen J, et al., 2019. Underwater image restoration based on a parallel convolutional neural network. *Remote Sens*, 11(13):1591. https://doi.org/10.3390/rs11131591

Wang SQ, Ma KD, Yeganeh H, et al., 2015. A patch-structure representation method for quality assessment of contrast changed images. *IEEE Signal Process Lett*, 22(12):2387-2390. https://doi.org/10.1109/LSP.2015.2487369

Wang Y, Zhang J, Cao Y, et al., 2017. A deep CNN method for underwater image enhancement. IEEE Int Conf on Image Processing, p.1382-1386. https://doi.org/10.1109/ICIP.2017.8296508

Wang Y, Song W, Fortino G, et al., 2019. An experimental-based review of image enhancement and image restoration methods for underwater imaging. *IEEE Access*, 7:140233-140251. https://doi.org/10.1109/ACCESS.2019.2932130

Wang YF, Wang HY, Yin CL, et al., 2016. Biologically inspired image enhancement based on retinex. *Neurocomputing*, 177:373-384. https://doi.org/10.1016/j.neucom.2015.10.124

Wang Z, Bovik AC, 2006. Modern Image Quality Assessment: Synthesis Lectures on Image, Video, and Multimedia

Processing. Morgan & Claypool, San Rafael, Argentina, p.1-156. https://doi.org/10.2200/S00010ED1V01Y200508IVM003

Wen HC, Tian YH, Huang TJ, et al., 2013. Single underwater image enhancement with a new optical model. IEEE Int Symp on Circuits and Systems, p.753-756. https://doi.org/10.1109/ISCAS.2013.6571956

Weng CC, Chen H, Fuh CS, 2005. A novel automatic white balance method for digital still cameras. IEEE Int Symp on Circuits and Systems, p.3801-3804. https://doi.org/10.1109/ISCAS.2005.1465458

Wu HD, Zhao M, Li FQ, et al., 2020. Underwater polarization-based single pixel imaging. *J Soc Inform Display*, 28(2): 157-163. https://doi.org/10.1002/jsid.838

Xie K, Pan W, Xu S, 2018. An underwater image enhancement algorithm for environment recognition and robot navigation. *Robotics*, 7(1):14. https://doi.org/10.3390/robotics7010014

Xu Q, Guo ZY, Tao QQ, et al., 2015. Transmitting characteristics of polarization information under seawater. *Appl Opt*, 54(21):6584-6588. https://doi.org/10.1364/AO.54.006584

Yang HY, Chen PY, Huang CC, et al., 2011. Low complexity underwater image enhancement based on dark channel prior. 2nd Int Conf on Innovations in Bio-inspired Computing and Applications, p.17-20. https://doi.org/10.1109/IBICA.2011.9

Yang M, Sowmya A, 2015. An underwater color image quality evaluation metric. *IEEE Trans Image Process*, 24(12): 6062-6071. https://doi.org/10.1109/TIP.2015.2491020

Yang M, Hu JT, Li CY, et al., 2019. An in-depth survey of underwater image enhancement and restoration. *IEEE Access*, 7:123638-123657. https://doi.org/10.1109/ACCESS.2019.2932611

Yemelyanov KM, Lin SS, Pugh EN, et al., 2006. Adaptive algorithms for two-channel polarization sensing under various polarization statistics with nonuniform distributions. *Appl Opt*, 45(22):5504-5520. https://doi.org/10.1364/AO.45.005504

Yin GJ, Liu B, Sheng L, et al., 2019. Semantics disentangling for text-to-image generation. Proc IEEE Conf on Computer Vision and Pattern Recognition, p.2327-2336. https://doi.org/10.1109/CVPR.2019.00243

You HF, Tian SW, Yu L, et al., 2020. Pixel-level remote sensing image recognition based on bidirectional word vectors. *IEEE Trans Geosci Remote Sens*, 58(2):1281-1293. https://doi.org/10.1109/TGRS.2019.2945591

Yuan MK, Peng YX, 2018. Text-to-image synthesis via symmetrical distillation networks. Proc 26th ACM Int Conf on Multimedia, p.1407-1415. https://doi.org/10.1145/3240508.3240559

Yuan MK, Peng YX, 2020. Bridge-GAN: interpretable representation learning for text-to-image synthesis. *IEEE Trans Circ Syst Video Technol*, 30(11):4258-4268. https://doi.org/10.1109/TCSVT.2019.2953753

Zhang S, Wang T, Dong JY, et al., 2017. Underwater image enhancement via extended multi-scale retinex. *Neurocomputing*, 245:1-9. https://doi.org/10.1016/j.neucom.2017.03.029

Zhang WD, Dong LL, Pan XP, et al., 2019a. Single image defogging based on multi-channel convolutional MSRCR. *IEEE Access*, 7:72492-72504. https://doi.org/10.1109/ACCESS.2019.2920403

Zhang WD, Dong LL, Pan XP, et al., 2019b. A survey of restoration and enhancement for underwater images. *IEEE Access*, 7:182259-182279. https://doi.org/10.1109/ACCESS.2019.2959560

Zhao MH, Hu CQ, Wei FL, et al., 2019. Real-time underwater image recognition with FPGA embedded system for convolutional neural network. *Sensors*, 19(2):350. https://doi.org/10.3390/s19020350

Zhao XW, Jin T, Qu S, 2015. Deriving inherent optical properties from background color and underwater image enhancement. *Ocean Eng*, 94:163-172. https://doi.org/10.1016/j.oceaneng.2014.11.036

Zhou JC, Hao ML, Zhang DH, et al., 2019a. Fusion PSPnet image segmentation based method for multi-focus image fusion. *IEEE Photon J*, 11(6):6501412. https://doi.org/10.1109/JPHOT.2019.2950949

Zhou JC, Zhang DG, Zou PY, et al., 2019b. Retinex-based laplacian pyramid method for image defogging. *IEEE Access*, 7:122459-122472. https://doi.org/10.1109/ACCESS.2019.2934981

Zhu JY, Park T, Isola P, et al., 2017. Unpaired image-to-image translation using cycle-consistent adversarial networks. Proc IEEE Int Conf on Computer Vision, p.2223-2232. https://doi.org/10.1109/ICCV.2017.244